# Nuclear spectroscopy of $^{189}$Os†

Dirck Benson, Jr.,* Peter Kleinheinz,‡ and R. K. Sheline
*Florida State University, Tallahassee, Florida 32306*

E. B. Shera
*Los Alamos Scientific Laboratory of the University of California, Los Alamos, New Mexico 87545*

(Received 14 June 1976)

Forty-three states have been observed up to an energy of 1474 keV in $^{189}$Os using the reactions $^{188}$Os$(d,p)^{189}$Os and $^{190}$Os$(d,t)^{189}$Os, produced with 12 MeV deuterons, and the $^{188}$Os$(n,\gamma)^{189}$Os reaction using thermal neutrons and observing $\gamma$ rays from 36 to 5933 keV. The neutron separation energy of $^{189}$Os was determined to be $5920.8 \pm 2.0$ keV in agreement with the value of the $(d,p)$ reaction. The $Q$ value for the $^{190}$Os$(d,t)^{180}$Os reaction was measured to be $-1530 \pm 4$ keV. Using $l$-transfer results, spin-parities were assigned to 14 states. A number of states up to 818 keV were qualitatively interpreted in terms of the Nilsson model. Anomalous Nilsson systematics particularly of the 1/2−[510] and 3/2−[512] bands involving anomalously large $(d,p)$ and $(d,t)$ cross sections populating the 5/2− and 3/2− states at 69.6 and 95.3 keV, respectively, are interpreted in terms of decreasing deformation and the consequent increase in Coriolis coupling. The low lying 5/2− state at 276 keV is interpreted as the lowest rotational state built on the 9/2−[505] level at 30.8 keV. This implies triaxiality for this configuration.

[NUCLEAR REACTIONS $^{188}$Os$(d,p)$, $^{190}$Os$(d,t)$, $E=12.0$ MeV, measured $\sigma(\theta)$, DWBA analysis; $^{188}$Os$(n_{th},\gamma)$; deduced energies, $l$, $j\pi$ of $^{189}$Os levels.
NUCLEAR STRUCTURE Nilsson model applied to $^{189}$Os; evidence for triaxiality.]

## I. INTRODUCTION

Current interest in the spectroscopy of the osmium nuclei is due largely to the fact that osmium is the only element for which stable isotopes span the transition from well deformed prolate shapes in the lightest Os isotopes to shapes which are alternatively described theoretically as spherical, $\gamma$ unstable, triaxial, or oblate in the region around mass number 190. Although energy levels of the even isotopes, both in experiment[1] and theory have been extensively investigated, very little information can be found in the literature concerning the nuclear structure of the heavier odd mass isotopes of osmium. This research reports on the nuclear energy levels of $^{189}$Os and was undertaken with two main purposes: to help fill in the gaps in the systematic knowledge of the single particle structure, and to probe the applicability of current nuclear models for odd-$A$ nuclei in the transition region. Some results of this work have been reported in an earlier publication,[2] with emphasis on the anomalous spectroscopic systematics and the consequent structural conclusions. The nucleus $^{189}$Os was studied as a product of the neutron transfer reactions $^{188}$Os$(d,p)^{189}$Os and $^{190}$Os$(d,t)^{189}$Os which populate neutron hole and particle states in characteristic ways such that they can be identified. A similar study of $^{189}$Os by the Aarhus group utilizing the reactions $^{188}$Os$(d,p)$, $^{190}$Os$(d,t)$, and $^{189}$Os$(d,d')$ was made approximately simultaneously with this study.[3] They obtained similar results but interpreted them somewhat differently from the interpretation given in the present paper.

In addition to the charged particle data, supplementary information about low spin states in $^{189}$Os was obtained from neutron capture experiments performed at the Los Alamos Scientific Laboratory using the reaction $^{188}$Os$(n,\gamma)^{189}$Os.

The usual approach for interpretation of nuclear levels of odd-$A$ nuclei in transition regions involves comparison with the Nilsson model,[4,5] which has been so successful in predicting the properties of strongly deformed nuclei. For example the Nilsson model, with the addition of rotational-particle (Coriolis) coupling, has been applied successfully to the odd tungsten isotopes.[6] In the present work, an attempt to extend the application of the Nilsson model has been carried beyond tungsten to $^{189}$Os, and many energy levels in $^{189}$Os have recognizable patterns of excitation and cross section similar to those seen in the isotonic $^{187}$W. While it is felt that Nilsson orbitals comprising the major components of the wave functions have been identified for many of the observed states below 500 keV, the Nilsson model is clearly less appropriate in this transition region.

Considerable theoretical effort has been made to describe even transitional Os nuclei in terms

of triaxial deformation.[7] This theory agrees fairly well with experimental observations for the even Os nuclei. Attempts[8-11] to describe the nuclear properties of the odd-$A$ transitional nuclei in terms of triaxial symmetry have been beset both with theoretical difficulties and the lack of adequate experimental data, especially for the heavier odd-$A$ Os nuclei. This paper is a part of a systematic experimental investigation of the heavier odd-$A$ Os nuclei. Similar studies of $^{191}$Os and $^{193}$Os are in progress.

## II. EXPERIMENTAL TECHNIQUES AND RESULTS

### A. Targets

Various methods of producing Os targets were tried, but discarded in favor of the inefficient but reliable techniques[15] in which $OsO_4$ is fed directly into the ion source of the isotope separator. Even with the most careful tuning of the instrument, two weeks of running time and 10 g of $OsO_4$ were consumed in the preparation of a target containing a few micrograms of separated isotope. Only a single target was made for the isotopes 188 and 190.

Elastic scattering measurements indicated thickness of ~15 and 40 $\mu$g/cm$^2$ for the $^{188}$Os and $^{190}$Os targets, respectively. Because the thin targets required long exposure to the beam, relatively thick C target backings of ~100 $\mu$g/cm$^2$ were employed as a safety precaution in spite of a slight detrimental effect on resolution.

### B. Charged particle spectroscopy

Charged particle reaction studies were carried out with 12 MeV deuterons from the EN tandem Van de Graaff accelerator at Florida State University. Emergent particles were analyzed in a 6/5 scaled-up version of the Browne-Buechner spectrograph,[12] through the use of Kodak NTA 50 $\mu$m nuclear emulsions spring-fitted to the focal surface of the spectrograph.

The data were analyzed with a series of computer programs[13-17] which were used to compute particle energy, $Q$ value, excitation energy, cross section, resolution, and a list of possible impurities for each peak, as well as appropriate error estimates.

Studies of the $^{188}$Os$(d,p)^{189}$Os reaction were carried out at 20°, 30°, 40°, 45°, 55°, 60°, 75°, 95°, and 125° with resolution varying from 10–17 keV full width at half maximum (FWHM). The reaction $^{190}$Os$(d,t)^{189}$Os was studied at 75°, 90°, 95°, and 125° with resolutions from 14–21 keV FWHM.

### C. Thermal neutron capture spectroscopy

Study of the reaction $^{188}$Os$(n,\gamma)^{189}$Os was carried out using thermal neutrons from the Los Alamos Omega West reactor. This facility has been described by Jurney, Motz, and Vegors.[18] The separated target used in these measurements was obtained from Oak Ridge and consisted of 98 mg of $^{188}$Os with the following isotopic composition [% (mass no.)]: <0.01 (184), <0.1 (186), <0.1 (187), 87.7 (188), 6.69 (189), 3.24 (190), 2.35 (190). Studies of the $(n,\gamma)$ spectra of separated targets of $^{189}$Os, $^{190}$Os, and $^{192}$Os were also carried out in order to identify isotopic $\gamma$ impurities.

The $\gamma$-ray spectrum was studied in three energy ranges to optimize experimental resolution. Each energy range used a different experimental arrangement. In the highest energy range (3.3–6.0 MeV) $\gamma$ rays were observed in coincidence with two 511 ± 50 keV $\gamma$ rays (presumably annihilation photons). This pair spectrometer arrangement eliminated confusion among double escape, single escape, and full energy photon peaks.

The resolution of the Ge(Li) detector employed in the pair spectrometer was 6–7 keV (FWHM), for high energy $\gamma$ rays. Nitrogen $\gamma$ rays from a 2.75 g sample of melamine ($C_3N_6H_6$) were used for the intensity calibration, and both nitrogen and carbon emitted well-known high energy $\gamma$ rays suitable for energy calibration. Carbon target containers provided internal energy reference lines. Standard energy and intensity values were taken from the compilation of Marion.[19] The total cross section for capture of thermal neutrons by $^{14}$N was taken to be 75.0 ± 7.5 mb.[20]

In the intermediate energy range (100–1500 keV), $\gamma$ rays were recorded in the anticoincidence or "anti-Compton" mode. Only those events in the Ge(Li) detector which were not in coincidence with any photon in the surrounding NaI annulus were accepted by the analyzer. This technique greatly reduces the background in the spectra arising from Compton scattering. Detection resolution was 3 keV FWHM at 1 MeV.

After each intermediate energy anticoincidence run, the sample was shielded from neutrons, and a new spectrum was recorded. In this way $\gamma$ rays emitted by long-lived activities could be distinguished from $\gamma$ rays which promptly follow neutron capture. Only the $\gamma$ rays associated with the known Ir daughter nuclei were observed.

Very low energy (below 100 keV) $\gamma$ rays were detected with a 3 mm deep Si(Li) detector with no coincidence restrictions. The resolution was 0.5–0.9 keV FWHM.

An assortment of standard radioactive sources was used for energy and relative efficiency cali-

brations below 1500 keV. The efficiencies of the Ge(Li) and Si(Li) detectors were related through the intensities of the Os $K$ x rays observed with both systems. Absolute cross sections were determined relative to the intensity of the 412 keV transition in $^{198}$Hg following irradiation of $^{197}$Au. The cross section for the $^{197}$Au$(n,\gamma)^{198}$Au was taken to be $98.8 \pm 0.3$ b.[21]

### D. $(d,p)$, $(d,t)$, and $(n,\gamma)$ results

Examples of spectra from the reactions $^{188}$Os$(d,p)^{189}$Os and $^{190}$Os$(d,t)^{189}$Os are presented in Fig. 1. The spectra have been adjusted to a common excitation energy scale and have been arranged in a "mirror plot" to provide a visual indication of the relative particle or hole character of each state. The spectra shown were among the very best obtained in terms of resolution and counting statistics. Tails on the high excitation side of the peaks were caused by straggling of protons and tritons in the relatively thick carbon backings of the targets.

Although the energy matching of the proton and triton spectra was obvious, as can be seen in Fig. 1, excitation energies were not immediately apparent because the position of the very weakly populated ground state peak (No. 0) was not clear. However, the energy spacings of the strong peaks 3, 4, and 5 matched the spacings of the well-known levels at 69.3, 95.3, and 216.8 keV. With the energy scale thus tentatively established, some weaker peaks fell into place and the ground state position was confirmed.

Excitation energies and differential cross sections obtained from the fitting of the raw data are presented in Table I. Excitation energies have been measured relative to the strong, well resolved peak at 95.3 keV excitation. The error in the measurement of the target thickness, which

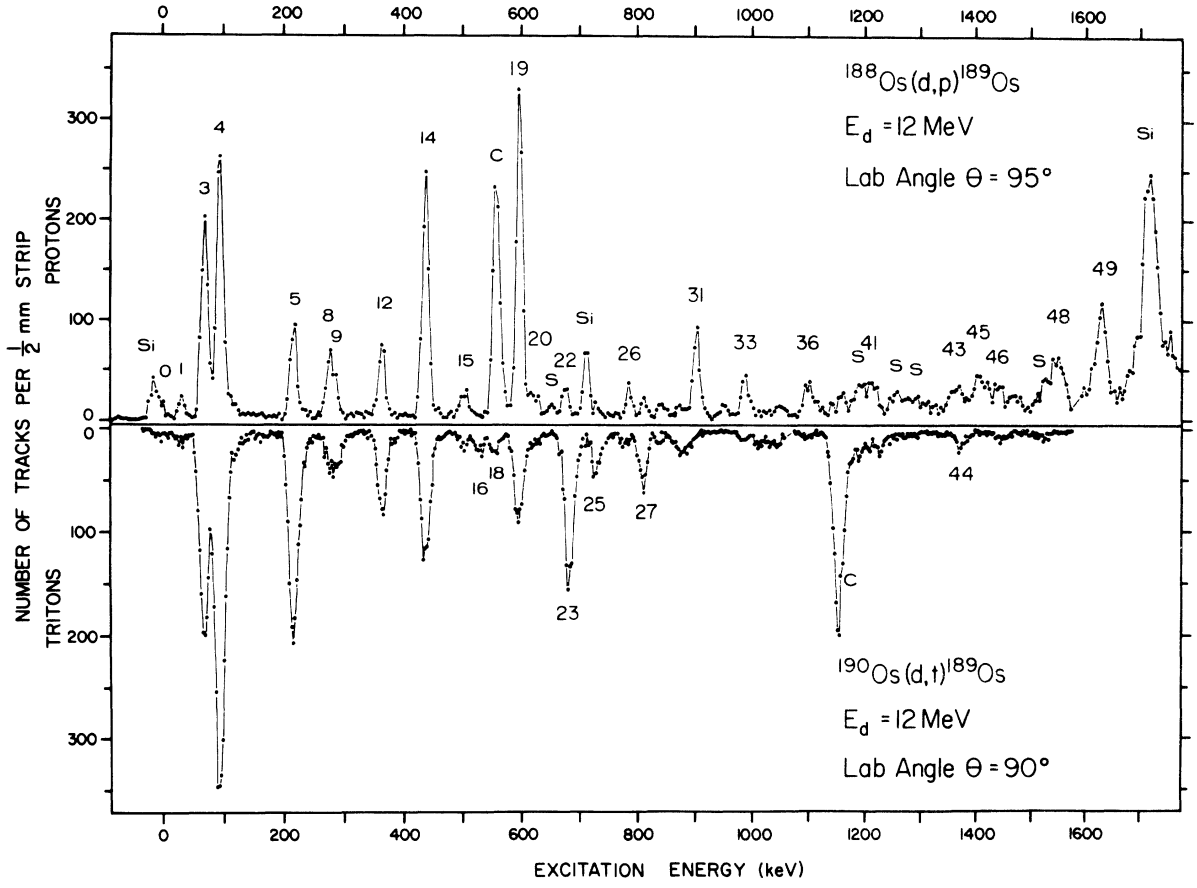


FIG. 1. Proton and triton energy spectra showing state populated in $^{189}$Os by the $(d,p)$ and $(d,t)$ reactions. Peak numbers correspond to energy levels listed in Table I. Peaks labeled C, Si, and S have been attributed to those elements. Vertical scales have been adjusted so that the peak at 70 keV excitation (No. 3) has the same height in both spectra; since this state is thought to be a member of the ground band with $U^2 \approx V^2$, peak heights provide a visual indication of relative particle or hole character.

TABLE I. Level energies and $(d,p)$ and $(d,t)$ differential cross sections for states in $^{189}$Os. Level numbers correspond to peaks in Figs. 1 and 3.

| Level No. | Adopted level energy (keV) | $d\sigma/d\Omega$ ($\mu$b/sr) $(d,p)$ 20° | 30° | 40° | 45° | 55° | 60° | 75° | 95° | 125° | $d\sigma/d\Omega$ ($\mu$b/sr) $(d,t)$ 75° | 90° | 95° | 125° | Reduced $d\sigma/d\Omega$ ($\mu$b/sr) $(d,p)$ 95° $Q=3$ MeV | $(d,t)$ 90° $Q=2$ MeV | Apparent $U^2$ | Inferred $l$ | Level No. |
|---|---|---|---|---|---|---|---|---|---|---|---|---|---|---|---|---|---|---|---|
| 0 | 0.00 | ••• | 31 | 21 | 18 | 31 | 30 | ••• | 13 | 6 | 7 | 14 | 6 | 5 | 16 | 10 | 0.6 | 1 | 0 |
| 1 | 30.81 [a] | ••• | ••• [b] | 23 | 20 | 19 | ••• | ••• | 21 | 11 | 12 | 23 | 30 | 17 | 26 | 16 | 0.5 | 5 | 1 |
| 2 | 36.23 ± 0.03 [c] | ••• | ••• | ••• | ••• | ••• | ••• | ••• | ••• | ••• | ••• | ••• | ••• | ••• | ••• | ••• | ••• | <3 [d] | 2 |
| 3 | 69.60 ± 0.07 [c] | 47 | 81 | 189 | 207 | 257 | ••• [b] | 354 | 213 | 97 | 214 | 348 | 432 | 171 | 262 | 252 | 0.48 | 3 | 3 |
| 4 | 95.35 ± 0.06 [c,e] | 476 | 332 | 386 | 518 | 619 | 689 | 437 | 303 | 118 | 428 | 671 | 708 | 260 | 370 | 497 | 0.40 | 1 | 4 |
| 5 | 216.8 [a] | 63 | 41 | 51 | 96 | 137 | 152 | 141 | 96 | 57 | 183 | 367 | 449 | 196 | 113 | 298 | 0.25 | 3 | 5 |
| 6 | 219.4 [a] | ••• | ••• | ••• | ••• | ••• | ••• | ••• | ••• | ••• | ••• | ••• | ••• | ••• | ••• | ••• | ••• | ••• | 6 |
| 7 | 233.6 [a] | ••• | ••• | ••• | ••• | ••• | ••• | ••• | ••• | ••• | ••• | ••• | ••• | ••• | ••• | ••• | ••• | ••• | 7 |
| 8 | 275.8 [a] | ••• [b] | 37 | 47 | 42 | 71 | 116 | ••• | 60 | 27 | ••• [b] | 63 | 94 | 14 | 69 | 54 | 0.54 | 3 | 8 |
| 9 | 290.5 ± 4.7 [f] | ••• [b] | ••• [b] | ••• | ••• | 13 | ••• | ••• | 31 | 21 | ••• [b] | 43 | 43 | 63 | 36 | 37 | 0.4 | 6 | 9 |
| 10 | 314.6 [a,g] | ••• | ••• | ••• | ••• | ••• | ••• | ••• | ••• | ••• | ••• | ••• | ••• | ••• | ••• | ••• | ••• | ••• | 10 |
| 11 | 346 ± 3 [h] | ••• | ••• | ••• | ••• | ••• | ••• | ••• | ••• | ••• | ••• | ••• | ••• | ••• | ••• | ••• | ••• | ••• | 11 |
| 12 | 365.7 ± 0.9 [f] | 38 | ••• [b] | 65 | 66 | 96 | 104 | ••• [b] | 79 | 44 | 64 | 133 | 153 | 65 | 88 | 122 | 0.40 | 3 | 12 |
| 13 | 424 ± 2 [h] | ••• | ••• | ••• | ••• | ••• | ••• | ••• | ••• | ••• | ••• | ••• | ••• | ••• | ••• | ••• | ••• | ••• | 13 |
| 14 | 439.1 ± 0.4 [c] | 316 | 208 | 208 | 315 | 434 | 505 | 369 | 243 | 87 | 137 | 220 | 252 | 80 | 265 | 214 | 0.52 | 1 | 14 |
| 15 | 506.0 ± 0.3 [c] | 42 | ••• [b] | ••• [b] | ••• [b] | 42 | ••• [b] | ••• | 34 | ••• [b] | 17 | 26 | 37 | 16 | 36 | 26 | 0.55 | 1 | 15 |
| 16 | 530.4 ± 1.5 [f] | ••• | ••• | ••• | ••• | ••• | ••• | ••• | ••• | ••• | 20 | 36 | 35 | 18 | ••• | 38 | 0 | <5 | 16 |
| 17 | 550.3 ± 0.4 [c] | ••• | ••• | ••• | ••• | ••• | ••• | ••• | ••• | ••• | ••• | ••• | ••• | ••• | ••• | ••• | ••• | <3 [d] | 17 |
| 18 | 557.6 ± 0.3 [c] | ••• [b] | ••• | ••• | ••• | ••• | 30 | ••• | ••• [b] | ••• | 20 | 40 | 46 | 14 | 20 [i] | 43 | 0.3 | <3 [d] | 18 |
| 19 | 599.7 ± 1.4 [f] | 476 | 292 | 275 | 389 | 541 | 587 | 449 | 310 | 119 | 88 | 158 | 194 | 69 | 321 | 172 | 0.62 | 1 | 19 |
| 20 | 621.7 ± 1.9 [f] | ••• | ••• | ••• | 30 | 31 | ••• | ••• | 26 | 28 | ••• | ••• | ••• | ••• | 27 | ••• | 1 | ••• | 20 |
| 21 | 671 ± 1 [h] | ••• | ••• | ••• | ••• | ••• | ••• | ••• | ••• | ••• | ••• | ••• | ••• | ••• | ••• | ••• | ••• | ••• | 21 |
| 22 | 679.4 ± 1.7 [f] | ••• | ••• [b] | ••• [b] | 58 | 50 | 65 | 36 | 28 | 22 | ••• | ••• | ••• | ••• | 28 | ••• | 1 | <5 | 22 |
| 23 | 688.4 ± 0.8 [f] | ••• | ••• | ••• | ••• | ••• | ••• | ••• | ••• | ••• | 148 | 254 | 281 | 113 | ••• | 306 | 0 | 1 | 23 |
| 24 | 716.9 ± 1.5 [f] | ••• | ••• | ••• | ••• | 48 | ••• [b] | ••• | ••• [b] | 20 | ••• | ••• | ••• | ••• | ~30 [i] | ••• | 1 | ••• | 24 |
| 25 | 735.1 ± 1.3 [f] | ••• | ••• | ••• | ••• | 18 | ••• | ••• | ••• | ••• | 36 | 71 | 99 | 37 | <10 | 90 | <0.1 | <5 | 25 |
| 26 | 786.4 ± 3.3 [f] | ••• | ••• | ••• | 39 | 19 | ••• | ••• | 21 | 22 | 12 | 22 | 21 | 18 | 20 | 29 | 0.4 | ••• | 26 |
| 27 | 817.8 ± 1.7 [f] | ••• | ••• | ••• [b] | ••• [b] | 20 | ••• | ••• | 13 | | 50 | 81 | 104 | 45 | 12 | 111 | 0.09 | <5 | 27 |
| 28 | 848.3 ± 1.9 [f] | ••• | ••• | ••• | ••• | 14 | ••• | ••• | 11 | ••• | ••• | ••• | ••• | ••• | 10 | ••• | 1 | ••• | 28 |
| 29 | 878.5 ± 3.4 [f] | ••• | ••• | ••• | ••• [b] | 9 | ••• | ••• | 8 | 22 | 10 | 32 | 32 | 26 | 8 | 46 | 0.1 | ••• | 29 |
| 30 | 898.2 ± 1.8 [f] | ••• | ••• | ••• | ••• | ••• | ••• | ••• | ••• | ••• | 18 | 31 | 39 | ••• [j] | ••• | 46 | 0 | ••• | 30 |
| 31 | 907.7 ± 1.9 [f] | ••• | 65 | 101 | 158 | 150 | 136 | 134 | 84 | 51 | ••• | ••• | ••• | ••• | 78 | ••• | 1 | 3 | 31 |
| 32 | 957.3 ± 2.4 [f] | ••• | ••• | ••• | ••• | 11 | ••• | ••• [b] | 8 | ••• | ••• | ••• | ••• | ••• | 7 | ••• | 1 | ••• | 32 |
| 33 | 993.4 ± 2.0 [k] | ••• | 45 | 45 | 70 | 80 | ••• [b] | ••• | 39 | 14 | 7 | 16 | 16 | 8 | 36 | 26 | 0.55 | 1 | 33 |
| 34 | 1028.5 ± 3.0 [f] | ••• | ••• | ••• | ••• | ••• | ••• | ••• | ••• | ••• | 5 | 24 | 48 | 26 | ••• | 41 | 0 | ••• | 34 |
| 35 | 1058.0 ± 3.9 [f] | ••• | ••• | ••• | ••• | 18 | ••• [b] | ••• | 9 | ••• | 19 | 27 | 36 | 21 | 8 | 47 | 0.6 | ••• | 35 |
| 36 | 1107.8 ± 1.8 [f] | ••• | ••• | ••• | 37 | 38 | ••• [b] | ••• | 40 | 38 | ••• | ••• | ••• | ••• | 35 | ••• | 1 | ••• | 36 |
| 37 | 1130 [h] | ••• | ••• | ••• | ••• | ••• | ••• | ••• | ••• | ••• | ••• | ••• | ••• | ••• | ••• | ••• | ••• | ••• | 37 |
| 38 | 1163.0 ± 3.8 [f] | ••• | ••• | ••• | 26 | 51 | 70 | ••• | 24 | ••• | 7 | ••• [b] | ••• | 13 | 21 | ~20 [i] | 0.5 | ••• | 38 |
| 39 | 1188.0 ± 1.8 [f] | ••• | ••• | ••• | 26 | 41 | 81 | ••• | ••• [b] | 21 | ••• | ••• | ••• | ••• | ~40 [i] | ••• | 1 | ••• | 39 |

TABLE I. *(Continued)*

| Level No. | Adopted level energy (keV) | $d\sigma/d\Omega$ ($\mu$b/sr) $(d,p)$ 20° | 30° | 40° | 45° | 55° | 60° | 75° | 95° | 125° | $d\sigma/d\Omega$ ($\mu$b/sr) $(d,t)$ 75° | 90° | 95° | 125° | Reduced $d\sigma/d\Omega$ ($\mu$b/sr) $(d,p)$ 95° $Q=3$ MeV | $(d,t)$ 90° $Q=2$ MeV | Apparent $U^2$ | Inferred $l$ | Level No. |
|---|---|---|---|---|---|---|---|---|---|---|---|---|---|---|---|---|---|---|---|
| 40 | 1210.5 ± 3.9 [f] | ··· | ··· | ··· | ··· | ··· | ··· | ··· | ··· | ··· | 14 | 49 | 40 | 21 | ··· | 102 | 0 | ··· | 40 |
| 41 | 1220.2 ± 2.0 [f] | ··· | ··· | ··· | 30 | 55 | ··· | ··· [b] | 42 | ··· [b] | ··· | ··· | ··· | ··· | 35 | ··· | 1 | ··· | 41 |
| 42 | 1242.8 ± 43 [f] | ··· | ··· | ··· | ··· | ··· | ··· | ··· | ··· | ··· | 11 | 40 | 51 | 18 | ··· | 87 | 0 | ··· | 42 |
| 43 | 1374.7 ± 1.5 [c] | ··· | ··· | ··· [b] | 19 | 19 | ··· | ··· [b] | 46 | ··· | ··· | ··· | ··· | ··· | 37 | ··· | 1 | <3 [d] | 43 |
| 44 | 1394.2 ± 2.0 [c] | ··· | ··· | ··· | ··· | ··· | ··· | ··· | ··· | ··· | 18 | 28 | 36 | 19 | ··· | 74 | 0 | <3 [d] | 44 |
| 45 | 1411.3 ± 2.0 [f] | ··· | ··· | ··· | ··· | 78 | ··· | ··· | 66 | ··· | ··· | ··· | ··· | ··· | 52 | ··· | 1 | ··· | 45 |
| 46 | 1445.5 ± 2.0 [f] | ··· | ··· | ··· | ··· | 48 | ··· | ··· | 43 | ··· | ··· | ··· | ··· | ··· | 34 | ··· | 1 | ··· | 46 |
| 47 | 1474.0 ± 3.0 [k] | ··· | ··· | ··· | 54 | 46 | ··· | ··· | 29 | ··· | ··· | ··· | ··· | ··· | 22 | ··· | 1 | <3 [d] | 47 |
| 48 | 1554.6 ± 2.5 [f] | ··· | ··· | ··· | 58 | 99 | ··· | 67 | 99 | 63 | ··· | ··· | ··· | ··· | 75 | ··· | 1 | ··· | 48 |
| 49 | 1633.7 ± 2.3 [f] | ··· | ··· | ··· | ··· [b] | ··· [b] | ··· [b] | 190 | 186 | 70 | ··· | ··· | ··· | ··· | 137 | ··· | 1 | ··· | 49 |
| 50 | 1699.6 ± 2.0 [c] | ··· | ··· | ··· | 98 | 128 | ··· | 112 | 68 | 76 | ··· | ··· | ··· | ··· | 49 | ··· | 1 | <3 [d] | 50 |
| 51 | 1724.8 ± 2.1 [f] | ··· | ··· | ··· | 432 | 486 | ··· | 529 | 511 | 261 | ··· | ··· | ··· | ··· | 364 | ··· | 1 | ··· | 51 |
| 52 | 1895.6 ± 3.0 [c] | ··· | ··· | ··· | ··· | ··· | ··· | ··· | ··· | ··· | ··· | ··· | ··· | ··· | ··· | ··· | ··· | < 3 [d] | 52 |
| 53 | 1941.1 ± 3.0 [c] | ··· | ··· | ··· | ··· | ··· | ··· | ··· | ··· | ··· | ··· | ··· | ··· | ··· | ··· | ··· | ··· | <3 [d] | 53 |

[a] Energy measured in $\beta$ decay, as given in Ref. 1.
[b] Obscured by known impurity.
[c] Energy determined from $(n, \alpha)$, averaged over as many cascades as possible.
[d] Limit inferred from primary $(n, \alpha)$ population.
[e] All excitation energies in $(d,p)$ and $(d,t)$ spectra measured relative to 95.35 keV state.
[f] Weighted average over all $(d,p)$ and $(d,t)$ measurements.
[g] Probably spurious; see text, and Ref. 33.
[h] Energy reported for $(d,d')$ reaction in Ref. 3.
[i] Obscured at $Q$-reduction angle; intensity estimated from measurements at other angles.
[j] Obscured at plate edge.
[k] Weighted average of $(d,p)$, $(d,t)$, and primary $(n, \alpha)$ measurements.

determines the cross section normalization between different angles, can be quite large ($\leq 20\%$ for strong states) because of the possible inhomogeneities in the isotope separator produced targets. The uncertainties of relative cross sections within any one spectrum are estimated to be about 10% strongly populated and well resolved peaks. In many cases, where the cross sections are extracted from weakly populated or composite groups, the uncertainty might well be as large as a factor of 2.

Also included in Table I are adopted values, for the orbital angular momentum transfer ($l$), which were extracted from the experimental angular distributions. For the $^{188}$Os$(d,p)^{189}$Os reaction data, the $l$ values were largely determined from comparison with theoretical angular distributions calculated according to the distorted wave Born approximation (DWBA).[22] For example, Fig. 2 shows the measured $(d,p)$ angular distributions for the strongly populated levels at 70 and 95 keV excitation; they are in good agreement with DWBA predictions calculated for the previously well established spin and parity assignments of $\frac{5}{2}-$ and $\frac{3}{2}-$, respectively.

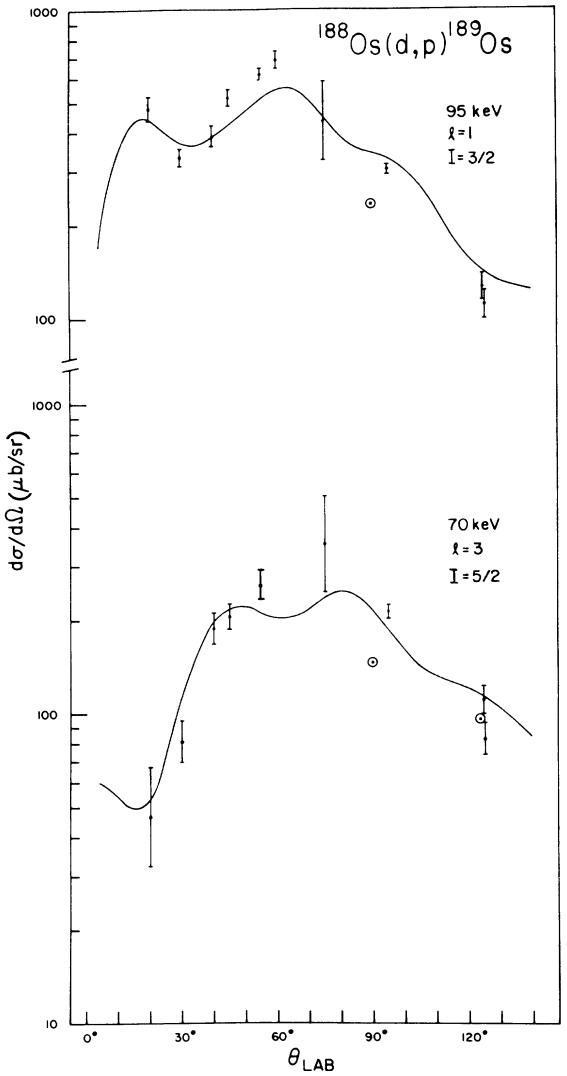


FIG. 2. Measured $(d,p)$ angular distributions for the 95 keV $\frac{3}{2}-$level and the 70 keV $\frac{5}{2}-$level in $^{189}$Os. Circles represent data taken from Ref. 3. For comparison, the results of the DWBA calculations for $l=1$ and $l=3$ are shown as solid lines with arbitrary vertical scale.

The $(d,t)$ data were in relatively poor agreement with the DWBA calculations, probably because of the difficulties in normalization. Nevertheless, an empirical comparison of observed angular distributions between states of known and unknown $l$ value made it possible to determine $l$ within ±1 unit.

The high energy $\gamma$-ray spectrum is shown in Fig. 3, and $\gamma$-ray energies and intensities are summarized in Table II. The total cross section for capture of thermal neutrons by $^{188}$Os is not known. However, the observed partial cross sections for $\gamma$ rays deexciting the capture state give a lower

TABLE II. High energy $\gamma$ rays observed in the $^{188}$Os$(n,\gamma)^{189}$Os experiment. Numbers in the "Assignment" column correspond to peaks in Fig. 3 and levels in Table I.

| $\gamma$-ray energy (keV) | Excitation energy (keV) | Intensity (mb) | Assignment |
|---|---|---|---|
| 5933.2 ± 3.0 | ··· | (40 ± 12) [a] | $^{189}$Os$(n,\gamma)^{190}$Os |
| 5884.5 ± 2.0 | 36.2 [b] | 136 ± 29 | 2 |
| 5562.0 ± 0.3 [c] | ··· | ··· | $^{14}$N$(n,\gamma)^{15}$N |
| 5533.0 ± 0.3 [c] | ··· | ··· | $^{14}$N$(n,\gamma)^{15}$N |
| 5481.6 ± 2.0 | 439.1 ± 0.6 | 119 ± 27 | 14 |
| 5414.9 ± 2.0 | 505.9 ± 0.6 | 311 ± 65 | 15 |
| 5370.2 ± 2.5 | 550.6 ± 0.7 | 97 ± 23 | 17 |
| 5363.3 ± 3.0 | 557.5 ± 0.8 | 31 ± 12 | 18 |
| 5297.4 ± 0.3 [c] | ··· | ··· | $^{14}$N$(n,\gamma)^{15}$N |
| 5268.5 ± 0.2 [c] | ··· | ··· | $^{14}$N$(n,\gamma)^{15}$N |
| 5147.1 ± 3.0 | ··· | (45 ± 18) [a] | $^{190}$Os$(n,\gamma)^{191}$Os |
| 4945.5 ± 0.2 [c] | ··· | ··· | $^{12}$C$(n,\gamma)^{13}$C |
| 4927.7 ± 3.0 | 993.1 ± 2.0 | 116 ± 42 | 33 |
| 4546.1 ± 2.5 | 1374.7 ± 1.5 | 118 ± 26 | 43 |
| 4526.6 ± 3.0 | 1394.2 ± 2.0 | 56 ± 18 | 44 |
| 4508.8 ± 0.3 [c] | ··· | ··· | $^{14}$N$(n,\gamma)^{15}$N |
| 4448.6 ± 4.0 | 1472.1 ± 3.0 | 35 ± 18 | 47 |
| 4221.2 ± 2.5 | 1699.6 ± 2.0 | 140 ± 36 | 50 |
| 4026.0 ± 4.0 | 1895.6 ± 3.0 | 37 ± 19 | 52 |
| 3980.5 ± 4.0 | 1941.1 ± 3.0 | 40 ± 20 | 53 |
| 3855.0 ± 2.0 [c] | ··· | ··· | $^{14}$N$(n,\gamma)^{15}$N |
| 3683.9 ± 0.2 [c] | ··· | ··· | $^{12}$C$(n,\gamma)^{13}$C |

[a] Relative intensity.

[b] All excitation energies were measured relative to this state.

[c] Energy taken from Ref. 19.

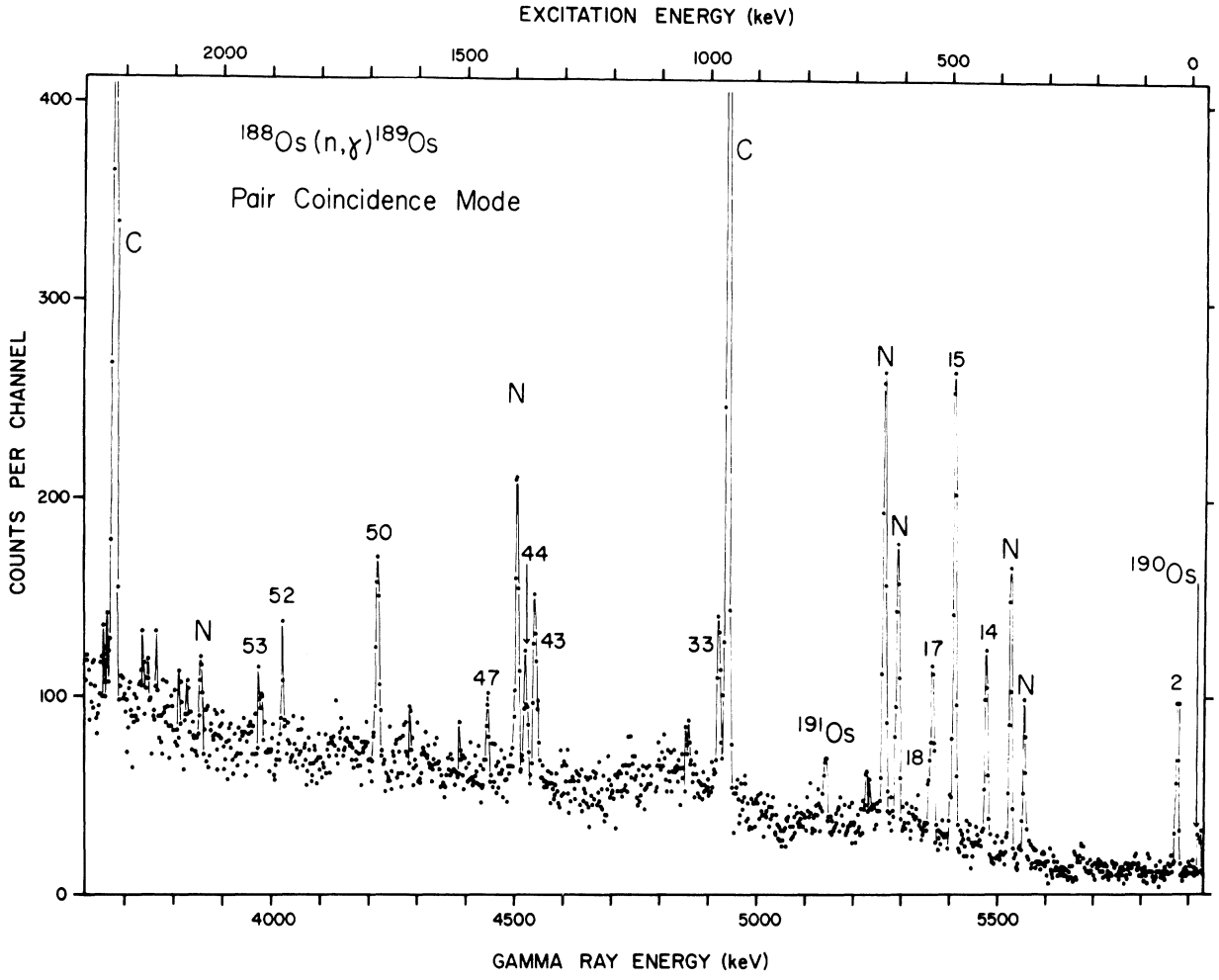


FIG. 3. High energy $\gamma$ ray spectrum observed following capture of thermal neutrons by $^{188}$Os. Peak numbers correspond to energy levels listed in Tables I and II. Peaks labeled C and N have been attributed to those elements. Peaks due to isotopic impurities are labeled with the mass number of the product.

limit of 1.2 b. The customary[18] energy weighted sum over $\gamma$ rays of all energies gives essentially the same value. Since this number is only a lower limit for the total capture cross section, it is appropriate to express the $\gamma$-ray intensities as partial cross sections for capture.

The sample was accidentally left open to the atmosphere during this 47 h run, so nitrogen lines were seen as well as carbon. These lines provided an internal energy calibration. Unfortunately, they could also have obscured some weak $^{189}$Os lines, but this work and other available data provide no indication that one should expect any $^{189}$Os lines at the nitrogen energies. The excitation energies listed in Table II were measured relative to the 36.2 keV level, as energy differences of the high energy $\gamma$ transitions.

The intermediate and low energy $\gamma$-ray spectra obtained with the Ge(Li) and Si(Li) detectors are shown in Figs. 4 and 5, respectively. Energies, cross sections, and transition assignments are given in Table III. The small amounts of $^{187}$Os and $^{189}$Os in the target material produced some of the stronger lines in the low energy spectrum, but these were readily identified. $\gamma$-ray lines which occurred with similar intensities in all Os targets have been labeled as impurities.

### E. Reaction $Q$ values

Transfer reactions and neutron capture studies are among the most precise methods for measurement of neutron separation energies, which determine relative nuclear masses. In neutron capture

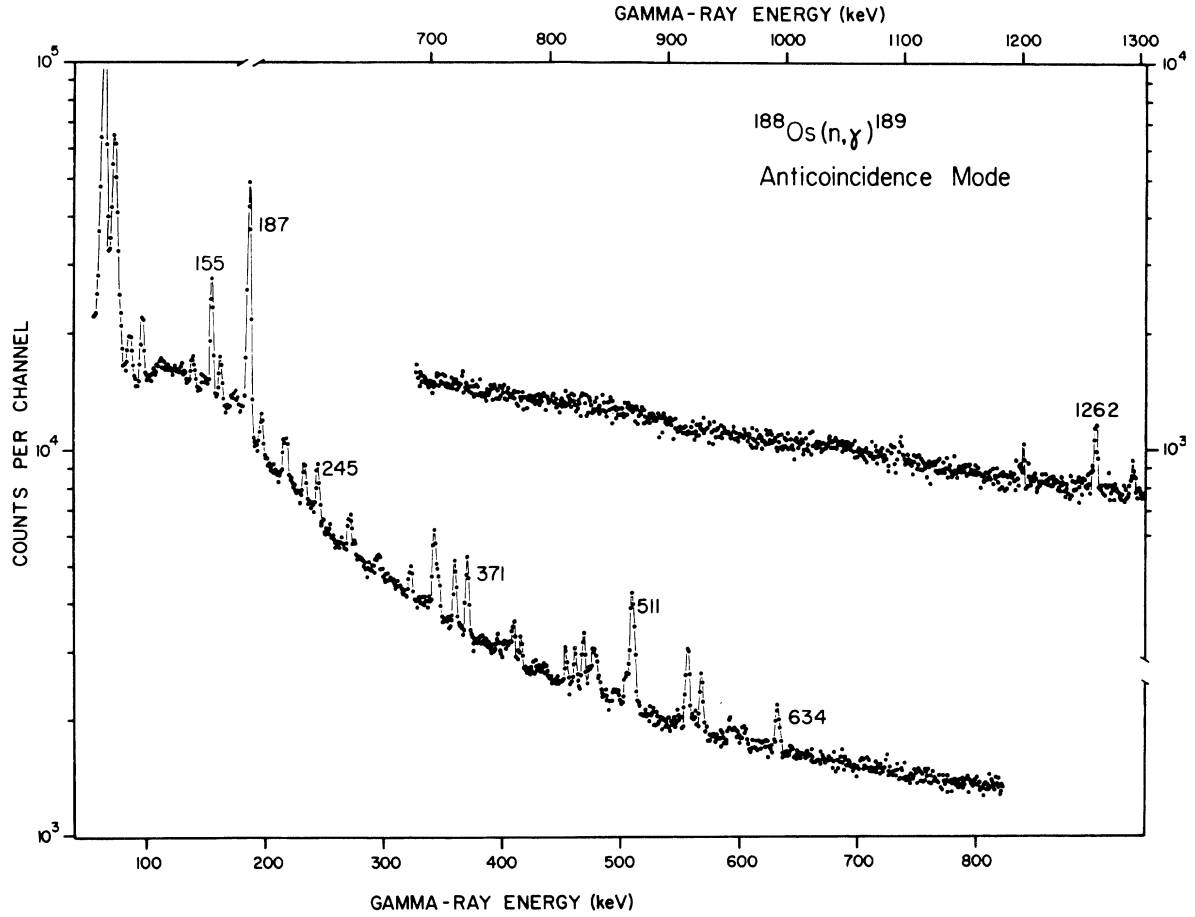


FIG. 4. Spectrum of $\gamma$ rays observed with the Ge(Li) detector, in anticoincidence with Compton scattered events in the surrounding NaI annulus. Energies and intensities of the peaks are listed in Table III.

studies the neutron separation energy $S_n$ is obtained directly as the excitation energy of the capture state. Neutron separation energies can also be determined by addition of $(d,p)$ $Q$ values to the deuteron binding energy, and by subtraction of $(d,t)$ $Q$ values from the triton $S_n$ value. Neutron separation energies obtained in these and other[3,23-27] experiments are compared in Table IV.

Values of $S_n$ for $^{189}$Os have been determined for all cascades from the capture state to the ground state. Where transition energies are known more precisely from conversion electron studies, those values have been used. The average result is $S_n = 5920.8$ keV. The standard deviation is less than 1 keV, but an error estimate of $\pm 2$ keV is assigned to include possible systematic errors.

Reference peaks were used for the refinement of $(d,p)$ and $(d,t)$ $Q$ values. The remarkably consistent values for the strong 95.3 keV state were averaged, and relative to those results the ground state $Q$ values were found to be $3694 \pm 4$ keV for $^{188}$Os$(d,p)^{189}$Os and $-1530 \pm 4$ keV for $^{190}$Os$(d,t)^{189}$Os. The corresponding $S_n$ values are given in Table IV.

### F. Level scheme

The previous knowledge of the level structure of $^{189}$Os was largely based on the electron capture decay[28,29] of $^{189}$Ir, and on complementary studies of the $\beta$ decay[30,31] of $^{189}$Re. These results were compiled by Artna.[32]

The level scheme based on the experimental $(n,\gamma)$ and charged particle results of this experiment is presented in Fig. 6. It had earlier been supposed that two very closely spaced $\frac{7}{2}-$ levels occur in $^{189}$Os at 217 and 219 keV.[32] Our low energy $(n,\gamma)$ spectra indicate $\gamma$ rays at 216.7 and 219.4 keV which suggest the existence of a close lying doublet at 216.7 and 219.4 keV, which depopulates to the ground state. We see a strong state in both the $(d,p)$ and $(d,t)$ spectra at this energy with an angular distribution consistent with $l = 3$, but we

cannot resolve this close lying doublet in our neutron transfer spectra. Preliminary results of a $\gamma$-$\gamma$ angular correlation study of Begzhanov *et al.*[34] indicate $\frac{5}{2}-$ for the 217 keV state. However, no final report of this work has appeared. In Fig. 6 we adopt the conclusions of Artna[32] suggesting two very close lying $\frac{7}{2}-$ levels. The neutron transfer data show a new level at 290 keV with $l=6$. A firm $\frac{13}{2}+$ assignment can be made for this level from the results of a recent $(\tau,\alpha)$ study.[35] Our data confirm the previously known levels,[44] up to 276 keV. A recent investigation[33] of electron capture in $^{189}$Ir has suggested that the level at 314.7 keV of Ref. 29 was probably spurious and also proposed the existence of a new level at 438.5 keV. Both of these changes are supported by the results of the present experiment. For every level below 1500 keV excitation, not established by a primary capture $\gamma$ ray, there is independent evidence from either the charged particle data or from low energy $\gamma$ deexcitation. No new levels based purely upon energy sums of low energy $\gamma$ rays have been proposed.

There are several transitions for which placement in the level scheme should be discussed. Relative intensities of the 245 and 59 keV $\gamma$ rays depopulating the 276 keV level[33] imply that the 59 keV transition must be placed between the 95 and 36 keV levels in the $(n,\gamma)$ level scheme.

The 219 keV $\gamma$ ray can be placed in the unusual position of feeding itself, 439 to 219 keV and 219 keV to the ground state. In the $^{189}$Ir decay, the 150 keV transition depopulates the 219 keV level with 16% of the $\gamma$ intensity of the 219 keV transition.[33] The fact that the 150 keV $\gamma$ ray was not seen at all in the $(n,\gamma)$ reaction indicates that not

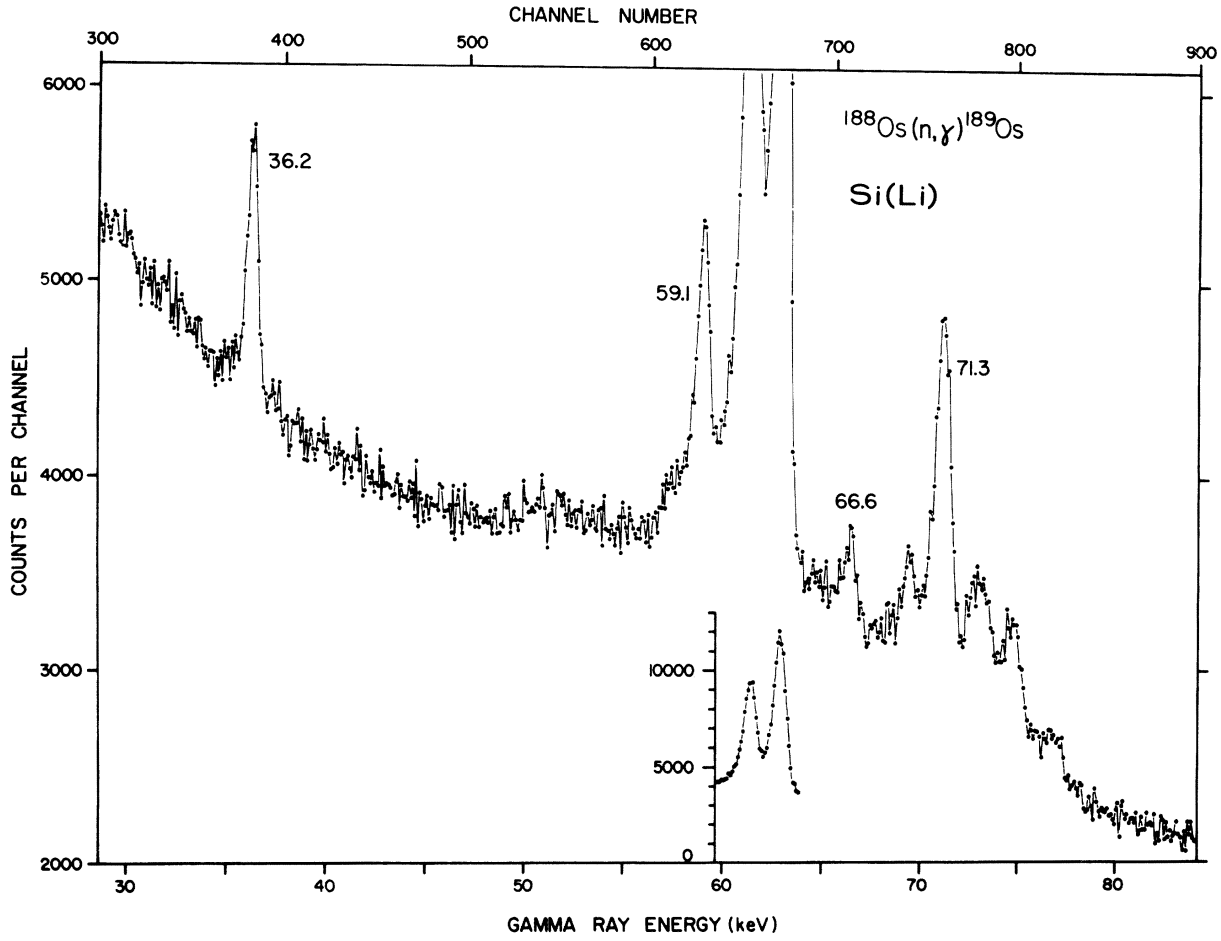


FIG. 5. Spectrum of low energy $\gamma$ rays, observed with the Si(Li) detector, following capture of thermal neutrons by $^{188}$Os. Peak energies and intensities are listed in Table III.

TABLE III. $\gamma$-ray transitions below 1300 keV, as observed in the spectra of Figs. 4 and 5. Intensities are given as partial cross sections for $\gamma$ ray production only; internal conversion has not been considered. Numbers in parentheses are relative intensities. $\gamma$ rays which occurred with equal intensity for all Os targets are designated as impurities.

| $\gamma$-ray energy (keV) | Intensity (mb) | Assignment | $\gamma$-ray energy (keV) | Intensity (mb) | Assignment |
|---|---|---|---|---|---|
| 36.23 ± 0.03 | 35 ± 10 | 36 → g.s. | 346.8 ± 0.5 | 96 ± 21 | ... |
| 59.12 ± 0.05 | 95 ± 28 | 95 → 36 | 361.1 ± 0.4 | (157) | $^{189}$Os$(n,\gamma)^{190}$Os |
| 61.55 ± 0.07 | (587) | Os $K\alpha_2$ x ray | 371.4 ± 0.4 | (203) | $^{189}$Os$(n,\gamma)^{190}$Os |
| 63.03 ± 0.07 | (796) | Os $K\alpha_1$ | 397.2 ± 0.7 | (39) | $^{189}$Os$(n,\gamma)^{190}$Os |
| 66.60 ± 0.07 | 39 ± 12 | 506 → 439 | 403.3 ± 0.6 | 38 ± 10 | 439 → 36 |
| 69.60 ± 0.07 | 70 ± 36 | 70 → g.s. | 407.2 ± 0.7 | (42) | $^{189}$Os$(n,\gamma)^{190}$Os |
| 71.3 ± 0.1 | (297) | Os $K'\beta_1$ | 410.6 ± 0.5 | 109 ± 24 | 506 → 95 |
| 73.2 ± 0.4 | (193) | Os $K'\beta_2$ + Pb $K\alpha_2$ | 416.5 ± 0.8 | (69) | Impurity |
| 74.9 ± 0.3 | (92) | Bi $K\alpha_2$ + Pb $K\alpha_1$ | 454.6 ± 0.4 | 111 ± 24 | 550 → 95 |
| 76.9 ± 0.3 | (43) | Bi $K\alpha_1$ | 462.4 ± 0.4 | 122 ± 27 | 558 → 95 |
| 85.7 ± 0.3 | (58) | Impurity | 469.9 ± 0.4 | 216 ± 45 | 506 → 36 |
| 95.9 ± 0.3 | (63) | 95 → g.s., + Imp | 474.7 ± 1.0 | 96 ± 29 | ... |
| 139.1 ± 0.4 | (36) | 234 → 95, + Imp | 478.9 ± 0.7 | (216) | $^{187}$Os$(n,\gamma)^{188}$Os |
| 155.2 ± 0.3 | (220) | $^{187}$Os$(n,\gamma)^{188}$Os | 483.0 ± 1.1 | 65 ± 28 | ... |
| 162.8 ± 0.6 | (70) | 234 → 70, + Imp | 495.6 ± 0.6 | 45 ± 13 | ... |
| 175.5 ± 0.5 | (77) | $^{190}$Os$(n,\gamma)^{191}$Os | 498.9 ± 0.6 | 47 ± 13 | ... |
| 186.7 ± 0.3 | (917) | $^{189}$Os$(n,\gamma)^{190}$Os | 505.8 ± 0.5 | 151 ± 34 | 506 → g.s. |
| 197.6 ± 0.4 | 78 ± 17 | 234 → 36 | 511.0 ± 0.3 | (679) | Annihilation |
| 216.7 ± 0.5 | 68 ± 16 | 217 → g.s. | 557.9 ± 0.4 | (389) [a] | $^{189}$Os$(n,\gamma)^{190}$Os |
| 219.4 ± 0.5 | 83 ± 19 | 219 → g.s., 439 → 219 | 569.5 ± 0.4 | (241) | $^{189}$Os$(n,\gamma)^{190}$Os |
| 234.0 ± 0.4 | 72 ± 16 | 234 → g.s. | 594.9 ± 0.8 | 146 ± 38 | ... |
| 245.2 ± 0.3 | 106 ± 23 | 276 → 234 | 605.1 ± 0.8 | (109) | $^{189}$Os$(n,\gamma)^{190}$Os |
| 272.4 ± 0.5 | 87 ± 20 | 506 → 234 | 633.8 ± 1.0 | (233) | $^{187}$Os$(n,\gamma)^{188}$Os |
| 275.9 ± 0.7 | 22 ± 9 | 276 → g.s. | 1097.5 ± 1.0 | (158) | Impurity |
| 296.5 ± 0.5 | 49 ± 13 | ... | 1262.2 ± 0.8 | (746) | $^{12}$C$(n,\gamma)^{13}$C |
| 323.6 ± 0.4 | 73 ± 16 | 558 → 234 | 1294.3 ± 1.0 | (316) | Impurity |
| 343.5 ± 0.4 | 217 ± 45 | 439 → 95 | | | |

[a] Relative intensities indicate that ~100 mb of an $^{189}$Os transition is buried under the strong 558 keV $^{190}$Os peak. It could connect the 588 keV level with the ground state.

all of the observed 219 keV intensity depopulates that level. Furthermore, the 219 keV level is so strongly populated in $^{189}$Ir decay that a small amount of 219 keV intensity deexciting the 439 keV level would not be noticeable in the intensity balance.

A comparison of the relative $\gamma$-ray intensities with those of the $^{189}$Os$(n,\gamma)^{190}$Os spectrum indicates that the peak at 558 keV probably includes ~100 mb of a $^{189}$Os transition as well as the well-known[24,25] strong 558 keV level with the ground state in $^{189}$Os.

Several $\gamma$ rays have not been placed in the level scheme. None of the unassigned transitions can form a simple closed energy loop with other known transitions in $^{189}$Os, neither with those observed in $(n,\gamma)$ nor with those known from radioactive decay. It is somewhat disturbing that a few unplaced transitions are relatively strong, especially the one at 595 keV, which carries 12% of the total capture intensity.

The 366 keV level, also unknown in radioactive decay, has $l = 3$. Spin and parity assignments are therefore expected to be $\frac{5}{2}-$ or $\frac{7}{2}-$.

Although the 439 keV state has been observed in $^{189}$Ir decay,[33] multipolarities have not been determined. Direct neutron capture and the $l = 1$ $(d,p)$ and $(d,t)$ angular distributions suggest $I\pi$

TABLE IV. Results of various neutron separation energy measurements.

| Nuclide | $S_n$ (keV) | | Technique | Reference |
|---|---|---|---|---|
| $^{189}$Os | 6002 | ±91 | Mass spectrometry | 23 |
| | 5921 | ±4 | Mass doublets | 26 |
| | 5914 | ±10 | $^{188}$Os$(d,p)^{189}$Os | 3 |
| | 5919 | ±4 | $^{188}$Os$(d,p)^{189}$Os | This work |
| | 5920.8 | ±2.0 | $^{188}$Os$(n,\gamma)^{189}$Os | This work |
| $^{190}$Os | 7771 | ±106 | Mass spectrometry | 23 |
| | 7794 | ±2 | Mass doublets | 26 |
| | 7798 | ±10 | $^{190}$Os$(d,t)^{189}$Os | 3 |
| | 7788 | ±4 | $^{190}$Os$(d,t)^{189}$Os | This work |
| | 7795 | ±5 | $^{189}$Os$(n,\gamma)^{190}$Os | 24 |
| | 7791 | ±3 | $^{189}$Os$(n,\gamma)^{190}$Os | 25 |
| | 7790 | ±3 | $^{189}$Os$(n,\gamma)^{190}$Os | 27 |

$=\frac{1}{2}-$ or $\frac{3}{2}-$. If he 439 keV level decays to the $\frac{7}{2}-$ 219 keV levl, as indicated by the dashed transition in Fi. 6, then $I\pi=\frac{3}{2}-$ would be required. Howevr, the 219.4 keV transition has been used elsehere in the level scheme. Therefore the $\frac{1}{2}-$ an$\frac{3}{2}-$ assignments are considered to be equally pbable.

The 506 and 93 keV states, like the 439 keV state, are popuated in the high energy $(n,\gamma)$ spectrum and have $l,p)$ angular distributions characteristic of $l=1$ tates. The suggested assignments are $I\pi=\frac{1}{2}-$ or $\frac{3}{2}-$. Other low spin $[\frac{1}{2},\frac{3}{2},(\frac{5}{2}+)]$ states are seenin the high energy $(n,\gamma)$ spectrum at 550, 558, 1?5 keV, and higher (Table III).

There are a w additional states for which $l$ values have ben inferred from the charged particle angular ditributions. The 908 and possibly the 679 keV levls have $l=3$, and $I\pi=\frac{5}{2}-$ or $\frac{7}{2}-$; the 600 keV state, with $l=1$, has $I\pi=\frac{1}{2}-$ or $\frac{3}{2}-$.

The log$ft$ values observed in $\beta$ decay to the $^{189}$Os daughter[32,33] are all consistent with the $I\pi$ assignments made in this section.

## III. NILSSON MODEL INTERPRETATION

### A. Calculated energy levels and spectroscopic factors

Theoretical energy levels and spectroscopic factors have been calculated in terms of Nilsson's deformable shell model,[4] including pairing effects. Several of the low lying states observed in $^{189}$Os resemble states predicted by the Nilsson model.

Single particle wave functions were derived from a modification[36] of Nilsson's Hamiltonian, which includes the effects of hexadecapole ($P_4$) as well as quadrupole ($P_2$) distortions. The coefficients

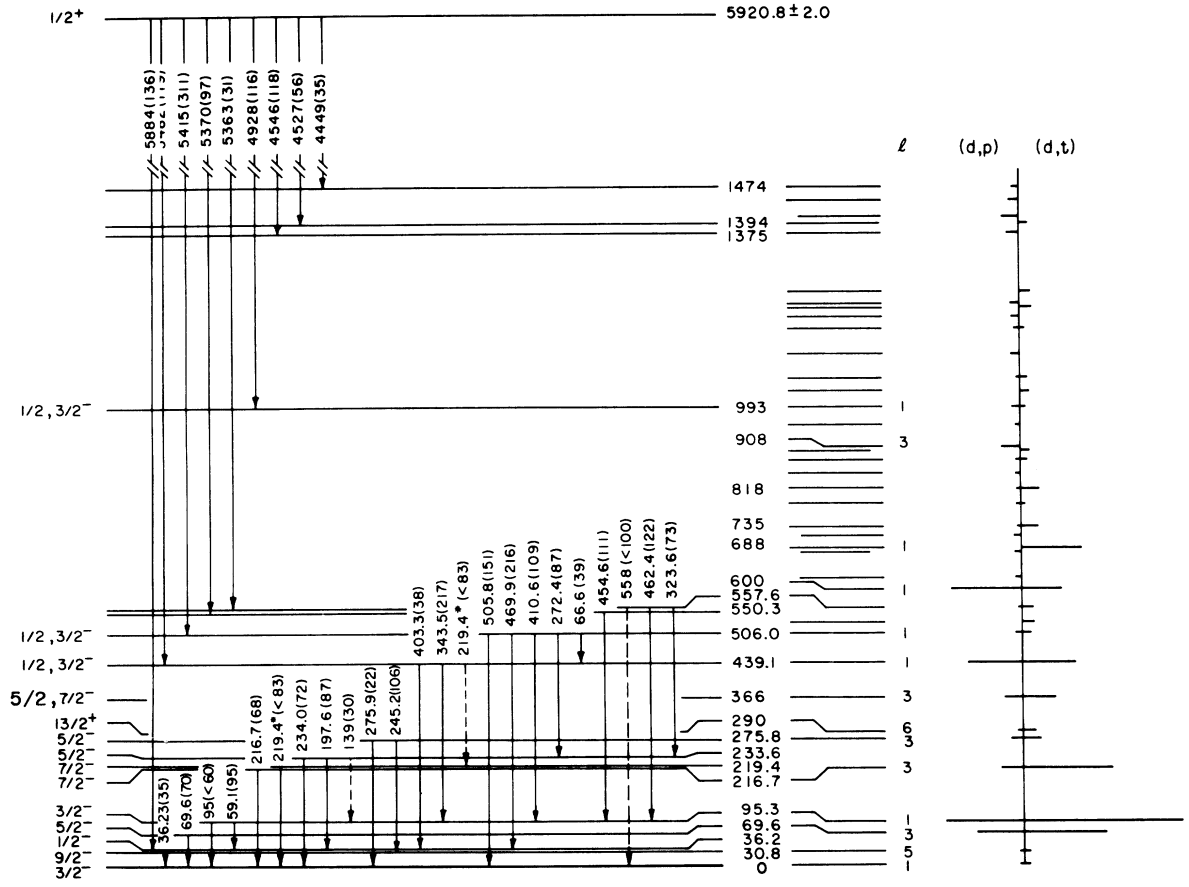


FIG. 6. Levelscheme for $^{189}$Os. Results of the $(n,\gamma)$ experiment are shown on the left, and levels populated in the transfer reactios are shown on the right. At the far right, bar lengths represent the differential cross sections measured at 95° or $(d,p)$ and 90° $(d,t)$. Dashed arrows represent transitions for which placement is uncertain. Asterisks indicate ouble placement.

$\kappa = 0.0636$ and $\mu = 0.393$ were taken from the work of Nilsson *et al.*[37]

Himmel[38] has measured the ground state nuclear quadrupole moment from hyperfine structure of the atomic spectrum of enriched $^{189}$Os, and obtained a value of $0.91 \pm 0.10$ b. If one assumes that the effective radius of nuclear charge is $R_0 = 1.20 \times 10^{-13} A^{1/3}$ cm, and neglects contributions of $P_4$ and higher components in the nuclear shape to the electric quadrupole moment, then this observed value corresponds[39] to a deformation of $\delta = 0.142 \pm 0.014$. By minimizing total potential energy with respect to deformation for even nuclei, Nilsson *et al.*[37] have predicted $\epsilon = 0.16$ for $^{190}$Os, and $\epsilon = 0.18$ for $^{188}$Os, with fairly constant $\epsilon_4 = 0.05$ for all Os isotopes. (For nuclei with relatively small deformations, the deformation parameters $\epsilon$ and $\epsilon_4$ in the stretched coordinate system are very nearly equal to the normal coordinate deformations $\delta$ and $\delta_4$.) The deformation parameters used in the present calculation were $\delta = 0.142$ and $\delta_4 = 0.050$. Variation of these parameters within reasonable limits did not appreciably improve agreement between theory and experiment.

To account for pairing correlations,[40] we have calculated quasiparticle energies ($E_{QP}$) from the Nilsson single particle energies ($E_P$) using a pairing gap, $2\Delta = 1.870$ MeV determined from known neutron binding energies. The Fermi energy $\lambda$ is expected to be close to the ingle particle energy for the 113th neutron level, about 49 MeV. Values for $\lambda$ and $\Delta$ were computed from the usual sum rules,[40] and the strength of the pairing interaction was adjusted until the known $\delta$ was reproduced. The final value for $\lambda$ was 4.285 MeV.

The occupation probability for a quasiparticle state is

$$V^2 = 1/2[1 - (E_{SP} - \lambda)/E_{QP}]. \quad (1)$$

The probability of a state being empty is

$$U^2 = 1 - V^2. \quad (2)$$

Theoretical excitation energies are given in Table V for all bandheads expected below 2 MeV

TABLE V. Calculated and observed bandhead energies (keV) for $^{189}$Os. The sign of $(U^2 - V^2)$ is given in parentheses to indicate the predominance of particle (+) or hole (−) character $a$ is the decoupling parameter of the $K = \frac{1}{2}$ bands.

| $K\pi[Nn_z\Lambda]$ | $E_{SP}$ | $E_{QP}$ | $a$ | Calculated excitation (keV) | Observed excitation (keV) |
|---|---|---|---|---|---|
| $\frac{1}{2}^-$ [510] | 49 135 | 947 | 0.722 | (−)0 | (−)36 |
| $\frac{1}{2}^-$ [521] | 48 030 | 1565 | 0.210 | (−)628 | (−)688 |
| $\frac{1}{2}^-$ [530] | 46 480 | 2956 | 4.679 | (−)1931 | |
| $\frac{1}{2}^-$ [501] | 52 205 | 3066 | 0.981 | (+)1995 | |
| $\frac{3}{2}^-$ [512] | 49 300 | 935 | | (+)22 | 0 |
| $\frac{3}{2}^-$ [501] | 51 230 | 2158 | | (+)1245 | |
| $\frac{5}{2}^-$ [512] | 47 090 | 2386 | | (−)1493 | |
| $\frac{5}{2}^-$ [503] | 51 628 | 2522 | | (+)1629 | |
| $\frac{7}{2}^-$ [503] | 48 718 | 1093 | | (−)211 | (−)217 |
| $\frac{7}{2}^-$ [514] | 47 638 | 1893 | | (−)1021 | |
| $\frac{9}{2}^-$ [505] | 49 543 | 969 | | (+)117 | (+)31 |
| $\frac{1}{2}^+$ [660] | 47 332 | 2165 | 6.921 | (−)1095 | |
| $\frac{1}{2}^+$ [651] | 52 052 | 2921 | 4.789 | (+)1892 | |
| $\frac{3}{2}^+$ [651] | 47 321 | 2175 | | (−)1263 | |
| $\frac{3}{2}^+$ [642] | 52 043 | 2912 | | (+)1999 | |
| $\frac{5}{2}^+$ [642] | 47 362 | 2138 | | (−)1246 | |
| $\frac{7}{2}^+$ [633] | 47 592 | 1934 | | (−)1061 | |
| $\frac{9}{2}^+$ [624] | 48 173 | 1453 | | (−)600 | (−) < 878 |
| $\frac{11}{2}^+$ [615] | 49 248 | 935 | | (−)103 | (−)31 < $E$ < 290 |
| $\frac{13}{2}^+$ [606] | 50 951 | 1910 | | (+)1098 | |

of excitation. Each band is designated by $K\pi[Nn_z\Lambda]$, where $N$, $n_z$, and $\Lambda$ are the familiar asymptotic quarum numbers for the Nilsson states. Table V also lists excitation energies for experimentally observed bandheads, the assignment of which will be discussed later. All Nilsson states expected below 1 MeV have at least tentatively been identified. Although the sequence is not correct, the bandhead energies have been predicted about as well as can be expected[41] in the transition region from this relatively simple model.

One of the most useful techniques for the identification of Nilsson states involves recognition of the characteristic "fingerprint" pattern of energies and intensities observed in single particle transfer reactions such as $(d,p)$ and $(d,t)$. A given Nilsson state generally has the same "fingerprint" from one strongly deformed nuclide to another. In a transition region the patterns change with deformation, but smooth trends aid identification.

The theoretical absolute differential cross section for stripping (+) or pickup (−) is given by the expression[41]

$$\frac{d\sigma^{\pm}}{d\Omega} = 2C_{jl}{}^2\Phi(\theta)\left(\frac{U}{V}\right)^2. \tag{3}$$

The spherical single particle cross section is

$$\Phi_l(\theta) = N\sigma_l(\theta), \tag{4}$$

where $\sigma_l(\theta)$ is the angular distribution function calculated from the distorted wave Born approximation[43] (DWBA), and $N$ is a normalization factor usually taken to be 1.50 for $(d,p)$ and 3.33 for $(d,t)$ reactions.[42]

For the $(d,p)$ angular distribution studies $\sigma_l(\theta)$ was calculated with optical model parameters which had been fitted to elastic scattering data. Siemssen and Erskine[44] have found that, although such parametes give reasonable angular distribution shapes, the calculated absolute cross sections are likely to be low by as much as 50% for deformed nuclei; it is better to use the tables of Perey[45] to estimate optical model parameters for a hypothetical spherical nucleus with the same mass and charge as the deformed nucleus being studied. Casten *et al.*[6] have obtained good agreement between theoretical and experimental cross sections for the W isotopes with optical model parameters derived from Perey's tables. Therefore, the tungsten $\Phi_l(90°)$ values of Casten *et al.*,[6] appropriately adjusted (Table VI), have been used in the calculation of absolute cross sections for $^{189}$Os.

It is necessary to consider the $Q$ dependence of $\Phi_l(\theta)$ when cross sections for various states are compared with theory and with each other. For convenience all cross sections have been put on a common basis by the $Q$-reduction technique of Elbek *et al.*,[6,42] whereby all cross sections are adjusted to the corresponding values at a standard $Q$ value somewhere in the middle of the observed range of $Q$, in this case 3.0 MeV for $(d,p)$ and −2.0 MeV for $(d,t)$. At a given angle, $\theta$, the $Q$ dependence of $\Phi_l(\theta)$ has about the same slope for all $l$ values. The slope changes very gradually with angle, and hardly at all with $Z$. Therefore, the W 90° average (over $l$) $Q$-reduction curves of Casten *et al.*[6] have been used for correcting the observed 95° Os$(d,p)$ and 90° Os$(d,t)$ cross sections to the standard $Q$ values (Table VI). The $\Phi_l(90°)$ values of Table VI also have been evaluated at the standard $Q$ values. For Os$(d,t)$ the W$\Phi_l(90°)$ values have been decreased by about 15% to correct for the strong $Z$ dependence[42] near the Coulomb barrier. For Os$(d,p)$ the $Z$ dependence correction is negligible, but the W$\Phi_l(90°)$ values have been corrected according to the ratio $\Phi_l(95°)/\Phi_l(90°)$ predicted in the earlier[22] DWBA angular distribution calculations. Hereafter, unless otherwise mentioned, all cross sections discussed will be $Q$-reduced cross sections at 95° for Os$(d,p)$ and at 90° for Os$(d,t)$.

TABLE VI. Differential single particle cross sections ($\mu$b/sr) used in the calculation of $d\sigma/d\Omega$ at the standard $Q$ values, $Q(d,p) = 3$ MeV and $Q(d,t) = -2$ MeV.

| $l$ | $\Phi_l(90°)$ [a] W$(d,p)$ | $\Phi_l(95°)$ Os$(d,p)$ | $\Phi_l(90°)$ [a] W$(d,t)$ | $\Phi_l(90°)$ Os$(d,t)$ |
|---|---|---|---|---|
| 0 | 923 | 821 | 870 | 757 |
| 1 | 585 | 556 | 567 | 493 |
| 2 | 531 | 483 | 489 | 425 |
| 3 | 228 | 196 | 203 | 177 |
| 4 | 164 | 159 | 133 | 116 |
| 5 | 34 | 35 | 27 | 23 |
| 6 | 17 | 17 | 12 | 10 |

[a] From Ref. 6.

The apparent $U^2$ values of Table I were calculated using the expression,

$$U^2 = \frac{(d\sigma^+/d\Omega)/\Phi_l^+}{(d\sigma^+/d\Omega)/\Phi_l^+ + (d\sigma - d\Omega)/\Phi_l^-}. \tag{5}$$

The experimental particle/hole designations of Table V were obtained from these apparent values of $U^2$.

Theoretical cross sections calculated from Eq. (3) are given in Table VII. The values of $C_{jl}{}^2$ and $U^2$ used[36] in the calculations are also tabulated. For comparison, the experimental cross sections for the states discussed in the next section are also given in the table.

TABLE VII. Comparison of theoretical and experimental cross sections for $^{189}$Os. The $Q$-reduced absolute differential cross sections were computed using Eq. (3), with $\Phi_l$ values taken from Table VI. Onishi's program DFWF (Ref. 36) was used for the Nilsson calculation ($C_{jl}^2$) and for the pairing calculation ($U^2$). The following parameters were used: $\delta = 0.14$; $\delta_4 = 0.05$, $\kappa = 0.0636$, $\mu = 0.393$, $\Delta = 935$ keV, and $\lambda = 49.285$ MeV.

| $IK[Nn_z\Lambda]$ | $C_{jl}^2$ | $U^2$ | $d\sigma/d\Omega$ ($\mu$b/sr), $Q$ reduced $(d,p)$ at 95° Calc. | Obs. | $(d,t)$ at 90° Calc. | Obs. | Observed excitation energy (keV) |
|---|---|---|---|---|---|---|---|
| $\frac{1}{2}\frac{1}{2}$[510] | 0.009 | 0.421 | 4 | <10 | 5 | <10 | 36 |
| $\frac{3}{2}\frac{1}{2}$[510] | 0.372 | | 174 | 370 | 212 | 497 | 95 |
| $\frac{5}{2}\frac{1}{2}$[510] | 0.457 | | 75 | <10 | 94 | <10 | 234 |
| $\frac{7}{2}\frac{1}{2}$[510] | 0.066 | | 11 | 88 | 14 | 122 | 366 |
| $\frac{9}{2}\frac{1}{2}$[510] | 0.082 | | 2.4 | | 2.2 | | ··· |
| $\frac{11}{2}\frac{1}{2}$[510] | 0.004 | | 0.1 | | 0.1 | | ··· |
| $\frac{1}{2}\frac{1}{2}$[521] | 0.331 | 0.099 | 36 | <10 | 294 | 306 | 688 |
| $\frac{3}{2}\frac{1}{2}$[521] | 0.343 | | 38 | <10 | 305 | 90 | 735 |
| $\frac{5}{2}\frac{1}{2}$[521] | 0.230 | | 9 | 12 | 73 | 111 | 818 |
| $\frac{7}{2}\frac{1}{2}$[521] | 0.060 | | 2.3 | 12 | 19 | | ··· |
| $\frac{9}{2}\frac{1}{2}$[521] | 0.030 | | 0.2 | | 1.2 | | ··· |
| $\frac{11}{2}\frac{1}{2}$[521] | 0.006 | | 0 | | 0.2 | | ··· |
| $\frac{1}{2}\frac{1}{2}$[530] | 0.001 | 0.026 | 0.0 | | 0.9 | | ··· |
| $\frac{3}{2}\frac{1}{2}$[530] | 0.000 | | 0.0 | | 0 | | ··· |
| $\frac{5}{2}\frac{1}{2}$[530] | 0.123 | | 1.2 | | 42 | | ··· |
| $\frac{7}{2}\frac{1}{2}$[530] | 0.008 | | 0.1 | | 2.7 | | ··· |
| $\frac{9}{2}\frac{1}{2}$[530] | 0.868 | | 1.6 | | 39 | | ··· |
| $\frac{11}{2}\frac{1}{2}$[530] | 0.000 | | 0 | | 0 | | ··· |
| $\frac{1}{2}\frac{1}{2}$[501] | 0.658 | 0.976 | 715 | | 15 | | ··· |
| $\frac{3}{2}\frac{1}{2}$[501] | 0.120 | | 131 | | 2.8 | | ··· |
| $\frac{5}{2}\frac{1}{2}$[501] | 0.188 | | 72 | | 1.6 | | ··· |
| $\frac{7}{2}\frac{1}{2}$[501] | 0.018 | | 7 | | 0.1 | | ··· |
| $\frac{9}{2}\frac{1}{2}$[501] | 0.015 | | 1.0 | | 0 | | ··· |
| $\frac{11}{2}\frac{1}{2}$[501] | 0.001 | | 0 | | 0 | | ··· |
| $\frac{3}{2}\frac{3}{2}$[512] | 0.186 | 0.508 | 105 | 16 | 90 | 10 | 0 |
| $\frac{5}{2}\frac{3}{2}$[512] | 0.656 | | 131 | 252 | 114 | 252 | 70 |
| $\frac{7}{2}\frac{3}{2}$[512] | 0.057 | | 11 | ··· | 10 | ··· | 219 |
| $\frac{9}{2}\frac{3}{2}$[512] | 0.097 | | 4 | | 2.2 | | ··· |
| $\frac{11}{2}\frac{3}{2}$[512] | 0.004 | | 0.1 | | 0.1 | | ··· |
| $\frac{3}{2}\frac{3}{2}$[501] | 0.712 | 0.951 | 752 | | 35 | | ··· |
| $\frac{5}{2}\frac{3}{2}$[501] | 0.213 | | 80 | | 4 | | ··· |
| $\frac{7}{2}\frac{3}{2}$[501] | 0.051 | | 19 | | 0.9 | | ··· |
| $\frac{9}{2}\frac{3}{2}$[501] | 0.022 | | 1.5 | | 0.1 | | ··· |

TABLE VII. *(Continued)*

| $IK[Nn_z\Lambda]$ | $C_{jl}^2$ | $U^2$ | $d\sigma/d\Omega$ ($\mu$b/sr), $Q$ reduced $(d,p)$ at 95° Calc. | Obs. | $(d,t)$ at 90° Calc. | Obs. | Observed excitation energy (keV) |
|---|---|---|---|---|---|---|---|
| $\frac{11}{2}\frac{3}{2}$ [501] | 0.002 | | 0.1 | | 0 | | ··· |
| $\frac{5}{2}\frac{5}{2}$ [512] | 0.006 | 0.040 | 0.1 | | 2.1 | | ··· |
| $\frac{7}{2}\frac{5}{2}$ [512] | 0.366 | | 6 | | 125 | | ··· |
| $\frac{9}{2}\frac{5}{2}$ [512] | 0.615 | | 1.7 | | 27 | | ··· |
| $\frac{11}{2}\frac{5}{2}$ [512] | 0.012 | | 0 | | 0.5 | | ··· |
| $\frac{5}{2}\frac{5}{2}$ [503] | 0.933 | 0.964 | 353 | | 12 | | ··· |
| $\frac{7}{2}\frac{5}{2}$ [503] | 0.021 | | 8 | | 0.3 | | ··· |
| $\frac{9}{2}\frac{5}{2}$ [503] | 0.045 | | 3 | | 0.1 | | ··· |
| $\frac{11}{2}\frac{5}{2}$ [503] | 0.001 | | 0.1 | | 0 | | ··· |
| $\frac{7}{2}\frac{7}{2}$ [503] | 0.834 | 0.241 | 79 | 113 | 224 | 298 | 217 |
| $\frac{9}{2}\frac{7}{2}$ [503] | 0.153 | | 2.6 | | 5 | | ··· |
| $\frac{11}{2}\frac{7}{2}$ [503] | 0.013 | | 0.2 | | 0.5 | | ··· |
| $\frac{7}{2}\frac{7}{2}$ [514] | 0.143 | 0.065 | 4 | | 47 | | ··· |
| $\frac{9}{2}\frac{7}{2}$ [514] | 0.843 | | 4 | | 36 | | ··· |
| $\frac{11}{2}\frac{7}{2}$ [514] | 0.014 | | 0.1 | | 0.6 | | ··· |
| $\frac{9}{2}\frac{9}{2}$ [505] | 0.994 | 0.633 | 44 | 26 | 17 | 16 | 31 |
| $\frac{11}{2}\frac{9}{2}$ [505] | 0.006 | | 0.3 | | 0.1 | | ··· |
| $\frac{1}{2}\frac{1}{2}$ [660] | 0.000 | 0.049 | 0 | | 0 | | ··· |
| $\frac{3}{2}\frac{1}{2}$ [660] | 0.000 | | 0 | | 0 | | ··· |
| $\frac{5}{2}\frac{1}{2}$ [660] | 0.000 | | 0 | | 0 | | ··· |
| $\frac{7}{2}\frac{1}{2}$ [660] | 0.000 | | 0 | | 0 | | ··· |
| $\frac{9}{2}\frac{1}{2}$ [660] | 0.038 | | 0.6 | | 8 | | ··· |
| $\frac{11}{2}\frac{1}{2}$ [660] | 0.000 | | 0 | | 0 | | ··· |
| $\frac{13}{2}\frac{1}{2}$ [660] | 0.961 | | 1.6 | | 18 | | ··· |
| $\frac{3}{2}\frac{3}{2}$ [651] | 0.000 | 0.048 | 0 | | 0 | | ··· |
| $\frac{5}{2}\frac{3}{2}$ [651] | 0.000 | | 0 | | 0 | | ··· |
| $\frac{7}{2}\frac{3}{2}$ [651] | 0.000 | | 0 | | 0 | | ··· |
| $\frac{9}{2}\frac{3}{2}$ [651] | 0.043 | | 0.7 | | 10 | | ··· |
| $\frac{11}{2}\frac{3}{2}$ [651] | 0.000 | | 0 | | 0 | | ··· |
| $\frac{13}{2}\frac{3}{2}$ [651] | 0.957 | | 1.6 | | 18 | | ··· |
| $\frac{5}{2}\frac{5}{2}$ [642] | 0.000 | 0.050 | 0 | | 0 | | ··· |
| $\frac{7}{2}\frac{5}{2}$ [642] | 0.000 | | 0 | | 0 | | ··· |
| $\frac{9}{2}\frac{5}{2}$ [642] | 0.046 | | 0.7 | | 10 | | ··· |
| $\frac{11}{2}\frac{5}{2}$ [642] | 0.000 | | 0 | | 0 | | ··· |
| $\frac{13}{2}\frac{5}{2}$ [642] | 0.954 | | 1.6 | | 18 | | ··· |

TABLE VII. *(Continued)*

| $IK[Nn_z\Lambda]$ | $C_{jl}^2$ | $U^2$ | $d\sigma/d\Omega$ ($\mu$b/sr), $Q$ reduced $(d,p)$ at 90° Calc. | Obs. | $(d,t)$ at 90° Calc. | Obs. | Observed excitation energy (keV) |
|---|---|---|---|---|---|---|---|
| $\frac{7}{2}\frac{7}{2}$ [633] | 0.000 | 0.062 | 0 | | 0 | | ··· |
| $\frac{9}{2}\frac{7}{2}$ [633] | 0.036 | | 0.7 | | 8 | | ··· |
| $\frac{11}{2}\frac{7}{2}$ [633] | 0.001 | | 0 | | 0 | | ··· |
| $\frac{13}{2}\frac{7}{2}$ [633] | 0.962 | | 2.0 | ··· | 18 | (41) | 1028? |
| $\frac{9}{2}\frac{9}{2}$ [624] | 0.016 | 0.117 | 0.6 | | 3 | | ··· |
| $\frac{11}{2}\frac{9}{2}$ [624] | 0.004 | | 0 | | 0.1 | | ··· |
| $\frac{13}{2}\frac{9}{2}$ [624] | 0.980 | | 4 | (8) | 17 | (46) | 878? |
| $\frac{11}{2}\frac{11}{2}$ [615] | 0.004 | 0.480 | 0.1 | | 0 | | ··· |
| $\frac{13}{2}\frac{11}{2}$ [615] | 0.996 | | 12 | 36 | 10 | 37 | 290 |
| $\frac{13}{2}\frac{13}{2}$ [606] | 1.000 | 0.936 | 32 | | 1.3 | | ··· |

### B. Nilsson levels

The ground state of $^{189}$Os, with spin and parity $\frac{3}{2}-$, has long been identified as the $\frac{3}{2}[512]$ bandhead. Its magnetic moment, +0.66 mm,[46] has the correct sign and roughly the magnitude expected for that Nilsson state. As can be seen in Table V, there is no other $\frac{3}{2}-$ bandhead expected at low energy. However, the experimental $(d,p)$ and $(d,t)$ cross sections to the ground state are much less than expected for the $\frac{3}{2}\frac{3}{2}[512]$ state. Furthermore, there are no higher band members which display the cross section pattern calculated for this band (Table VII). Coulomb excitation, which mainly populates ground state rotational band members by an $E2$ process, strongly excites the $\frac{5}{2}-$ 70 keV state[47,48] and the $\frac{7}{2}-$ 219 keV state.[49] If the 70 and 219 keV states are the $\frac{5}{2}-$ and $\frac{7}{2}-$ members of the ground state band, their spacing deviates strongly from the normal rotation spacing. The $\frac{3}{2}\frac{5}{2}$ spacing corresponds to an inertial parameter of $\hbar^2/2I = 13.9$ keV, while the $\frac{5}{2}\frac{7}{2}$ spacing gives $\hbar^2/2I = 21.4$ keV. For the $\frac{3}{2}[512]$ band the following systematic deviations from theory have been consistently established[6,50,51] for the neighboring $N > 109$ nuclei: The $\frac{3}{2}\frac{5}{2}$ energy separation is anomalously small, and the transfer cross sections to the $\frac{3}{2}$ and $\frac{7}{2}$ band members are very weak, whereas the $\frac{5}{2}$ member receives much larger cross section than calculated. The ground state, 70, and 219 keV states in $^{189}$Os strongly resemble the $\frac{3}{2}[512]$ band members observed in the neighboring nuclei. Therefore, we assign these levels as the three lowest members of the $\frac{3}{2}[512]$ band. All these deviations from theory have been attributed to Coriolis mixing,[6,51-53] which will be discussed later. If one assumes that the alternate deviation of levels from rotational spacings continues up the band, the inertial parameter $\hbar^2/2I = 18.3$ keV obtained from the $\frac{3}{2}\frac{7}{2}$ spacing gives estimates of the $\frac{5}{2}\frac{9}{2}$ and $\frac{7}{2}\frac{11}{2}$ spacings which predict the $\frac{9}{2}-$ level at 362 keV and the $\frac{11}{2}-$ level at 585 keV. The $\frac{9}{2}-$ and $\frac{11}{2}-$ members are not expected to have observable transfer cross sections, nor are they likely to be populated in $\beta$ decay. As ground state band members they might be populated by multiple Coulomb excitation, which has not been studied for $^{189}$Os, or by inelastic scattering, which generally favors collective excitations. The levels observed in the $(d,d')$ reaction[3] at 346 and 594 keV fit well the predictions for the $\frac{9}{2}-$ and $\frac{11}{2}-$ members of the $\frac{3}{2}[512]$ band.

It has long been recognized[54] that the $\frac{9}{2}-$ level at 31 keV is the $\frac{9}{2}[505]$ bandhead. The observed transfer cross section supports this assignment. The value of $C_{jl}^2$ indicates that essentially all of the $(d,p)$ and $(d,t)$ strength for this band goes to the $\frac{9}{2}-$ member. As expected, no higher member has been observed.

Although a possible spin of $\frac{3}{2}$ for the 36 keV level could not be excluded by model-independent reasoning, this state has been assigned as the $\frac{1}{2}[510]$ bandhead. Both the low excitation energy and the lack of transfer cross section for this state agree well with the predictions of the Nilsson model.[55] No other low spin states, except the $\frac{3}{2}[512]$ ground state, are expected at low energy. In a nuclear resonance absorption (Mössbauer) investigation, Wagner *et al.*[56] have found that the magnetic moment of the 36 keV level is $+0.23\mu_N$, similar to

that of the $\frac{1}{2}$[510] ground state in $^{187}$Os and $^{183}$W. It is expected that the Coriolis interaction between the $\frac{1}{2}$[510] and the $\frac{3}{2}$[512] will disrupt the structure of both bands. For the $\frac{1}{2}$[510] band just as in the case of the $\frac{3}{2}$[512] band, $^{189}$Os has a set of levels resembling the well established $\frac{1}{2}$[510] band members in neighboring $N>109$ nuclei, which fail to match the calculated pattern. The proposed set includes the levels at 36, 95, 234, and 366 keV. For the $\frac{1}{2}$[510] band the $\frac{3}{2}-$ and $\frac{7}{2}-$ members have transfer sections exceeding the theoretical values, while the $\frac{5}{2}-$ cross section is much smaller than calculated. The 36 and 234 keV states were not seen at all in $(d,p)$ and $(d,t)$, although a part of the small cross section assigned to the 31 keV state may belong to the unresolved 36 keV level. By far the strongest $\gamma$-ray and conversion electron transitions deexciting the 95 and 234 keV states are transitions within the proposed band. The energy spacings of the $\frac{1}{2}$, $\frac{3}{2}$, and $\frac{5}{2}$ members correspond to $\hbar^2/2I = 23.7$ keV with a decoupling parameter $a = -0.17$, while the $\frac{1}{2}$, $\frac{3}{2}$, and $\frac{7}{2}$ spacings $\hbar^2/2I = 23.1$ and $a = -0.15$. This good agreement of apparent rotational parameters supports the argument that these levels belong to a band. The apparent decoupled parameter follows the decreasing trend observed in neighboring nuclei[57] but bears no resemblance to the theoretical value $a = +0.72$. The observed rotational parameters indicate that the $\frac{9}{2}$ and $\frac{11}{2}$ members might lie at about 610 and 830 keV, respectively. Weak states at 620 and 973 keV are assigned in Ref. 3 as the $\frac{9}{2}$ and $\frac{11}{2}-$ members of the $\frac{1}{2}-$[510] band.

The $\frac{7}{2}-$ level at 217 keV has the excitation energy and cross sections expected for the $\frac{7}{2}$[503] bandhead. Higher members of this band are predicted to have small transfer cross sections, and they have not been seen.

The state at 290 keV, with $l=5$ or 6, has about the right energy and cross section to be the $\frac{13}{2}+$ member of the $\frac{11}{2}$[615] band. There are no strong $l=5$ states expected at low energy except for the $\frac{9}{2}$[505], which has already been placed at 31 keV. Kerek *et al.*[35] have given a very preliminary report of work in progress on the reaction $^{190}$Os($^3$He,$\alpha$)$^{189}$Os. From the excitation scale of their figure it can be seen that the strongest state in their spectrum ($\theta = 60°$) is at about 290 keV. This pickup reaction preferentially populates high spin hole states; $\Phi_l(\theta)$ is very small for $l<4$, and peaks at 60° for $l=6$.[28] Nilsson orbitals coming from the $i_{13/2}$ shell, such as the $\frac{11}{2}$[615], have nearly all of their $C_{jl}$ strength in the $\frac{13}{2}$ member; generally these $\frac{13}{2}+$ states give the strongest peaks in ($^3$He,$\alpha$) spectra.[58] Therefore, it is fairly certain that the 290 keV level is the $\frac{13}{2}$ member of the $\frac{11}{2}$[615] band. The $\frac{11}{2}$ member is expected to be weak in transfer reactions, and has not been observed in this work nor in the $(d,p)$ and $(d,t)$ spectroscopy of neighboring nuclei.[6,50,51] The $\frac{11}{2}+$ level is known to exist in some nearby odd-$N$ nuclei, having been observed in radioactive decay for example in $^{187}$Os at 257 keV.[59] In $^{189}$Os the $\frac{11}{2}$[615] bandhead is probably in the vicinity of 100 keV implying a somewhat Coriolis compressed rotational spacing. Certainly it is above the $\frac{9}{2}-$ level at 31 keV; otherwise the $\frac{9}{2}-$ would decay by an $E1$ transition to the $\frac{11}{2}+$, giving a long lived $M4$ isomer.

Other strong peaks in the ($^3$He,$\alpha$) spectrum[35] were observed at about 870 and 1020 keV. The lower one, possibly the same state seen in the $(d,t)$ reaction at 878 keV, is probably the $\frac{13}{2}+$ member of the $\frac{9}{2}$[624] band. This assignment would place the unobserved $\frac{9}{2}$[624] bandhead reasonably close to, but probably somewhat below, the Nilsson model estimate of 600 keV. The 1020 peak, possibly the same state seen in $(d,t)$ at 1028 keV, is probably the $\frac{13}{2}\frac{7}{2}$[633], although it could instead be the $\frac{13}{2}\frac{1}{2}$[660].

Although there are many levels below 1 MeV, some of them strongly populated, which have not yet been assigned, the Nilsson model calculations (Tables V and VII) predict only one further band below 1 MeV, the $\frac{1}{2}$[521] hole excitation. There are hole states in the $(d,t)$ spectrum at 688, 735, and 818 keV which have reasonable spacings for the first three members of a $K=\frac{1}{2}$ band. The $l$ values (Table I) inferred from the $(d,t)$ angular distributions are somewhat inconclusive, but they would permit the $\frac{1}{2}-$, $\frac{3}{2}-$, $\frac{5}{2}-$ spin sequence for these states. The rotational parameters are $\hbar^2/2I = 16.1$ keV and $a = +0.02$, which would place the unobserved $\frac{7}{2}$ member at around 928 keV. The theoretical value for the $\frac{1}{2}$[521] decoupling parameter is $a = +0.21$. The proposed band in $^{189}$Os resembles the $\frac{1}{2}$[521] band in the W isotopes[6] in that the $(d,t)$ intensity of the $\frac{3}{2}$ member is considerably smaller than the theoretical estimate. However, the spacings in W are quite different, with a $\approx 0.8$. This difference in spacings does not destroy the analogy between Os and W since our calculations[36] indicate that the decoupling parameter for the $\frac{1}{2}$[512] orbital is quite sensitive to deformation, especially to $\delta_4$. Although it seems possible to identify the 688, 735, and 818 keV levels with $\frac{1}{2}$, $\frac{3}{2}$, and $\frac{5}{2}$ members of the $\frac{1}{2}$[521] band, this assignment is quite speculative. A different assignment utilizing two strongly populated lower lying $l=1$ states is postulated in Ref. 3. We assign these lower states as members of $\gamma$ vibrational bands.

A computer program written by Onishi[36] has been used for Coriolis coupling calculations in an attempt to explain the perturbed band structure of

$^{189}$Os. This program considers mixing of all possible Nilsson states below some chosen energy cutoff. Although the calculations did not succeed in reproducing the experimentally observed spectra, they did correctly predict several trends.

The $\frac{1}{2}[510]$ and $\frac{3}{2}[512]$ bands interact strongly. The predicted directions of the deviations from normal rotational spacings are in agreement with the experiment. Mixing between the $\frac{3}{2}\frac{1}{2}[510]$ and the $\frac{3}{2}\frac{3}{2}[512]$ pushes the latter down, so that it lies below the $\frac{1}{2}\frac{1}{2}[510]$ and thus becomes the ground state contrary to the unperturbed prediction (Table V). With regard to theoretical $(d,p)$ and $(d,t)$ intensities, the mixed band members alternate between constructive and destructive interference, so that the $\frac{3}{2}\frac{1}{2}[510]$, the $\frac{5}{2}\frac{3}{2}[512]$, and the $\frac{7}{2}\frac{1}{2}[510]$ have much more than the unperturbed strength, while the other members are weakened by mixing. The measured cross sections clearly display the same alternate deviation from the unperturbed theoretical values (Table VII).

The $\frac{9}{2}\frac{9}{2}[505]$ mixes with the $\frac{9}{2}\frac{7}{2}[503]$, and thus is pushed to a lower energy than the unperturbed Nilsson model would predict. The $\frac{7}{2}\frac{7}{2}[503]$ remains fairly pure, staying at about the expected energy.

The mixing calculations do not predict that the $(d,t)$ strength of the $\frac{3}{2}[521]$ state should be diminished.

The existence of two $\frac{7}{2}-$ states only 2.7 keV apart at $\approx 218$ keV may also be understood on the basis of Coriolis coupling. Since $\Delta K = 2$ for $\frac{7}{2}\frac{7}{2}[503]$ and $\frac{7}{2}\frac{3}{2}[512]$ states, they will Coriolis mix only to second order with $K = \frac{5}{2}-$ bands. The only reasonable possibilities are $\frac{5}{2}[512]$ and $\frac{5}{2}[503]$ which occur at $\approx 1$ MeV and at several MeV, respectively. However, although in each case Coriolis coupling is large between one of the pairs, it is very small for the other pair implying a small second order Coriolis coupling between the observed $\frac{7}{2}-$ states.

The application of the prolate Nilsson model, with pairing, to the nuclear level structure of $^{189}$Os has been reasonably successful. For every Nilsson orbital expected below 1 MeV, at least one band member has been identified in the level scheme although the $\frac{1}{2}[521]$ assignment is much less certain than the other orbital identifications. Overall agreement between theoretical and observed energies and transfer intensities was fairly good for those levels which have been assigned. Several bands have perturbed patterns which indicate that band mixing is important; this is expected for a moderately deformed nucleus like $^{189}$Os since, in the Nilsson model, $K$ is a good quantum number only at large deformation. Coriolis mixing calculations improve agreement of theory with experiment. However, there are many levels, one as low as 276 keV, which have not been predicted by the model.

### C. Anomalous vibrational excitations

The most obvious failure of the predictions based upon the Nilsson model is the large number of states below 1 MeV in $^{189}$Os for which no explanation was provided. A related problem is the observation of states such as those at 439 and 600 keV which cannot be rotational members of the lowest lying axially symmetric Nilsson bands, but which still have $(d,t)$ intensities roughly comparable with their $(d,p)$ intensities. The pairing theory predicts that quasiparticle states with bandhead excitation energies of a few hundred keV or higher should have either predominantly particle or predominantly hole character. This prediction has been borne out by the Nilsson states identified in $^{189}$Os. Even the $\frac{7}{2}[503]$ at 217 keV has about 75% hole character.

The natural approach then is to consider whether the unassigned levels might be collective excitations built upon low lying quasiparticle states.

The simplest picture for a nonrotational collective excitation in an odd nucleus[60] is that of a quasiparticle coupled to a vibration of the even-even core. The one-phonon $2+\ \gamma$ vibration is the only collective excitation known to lie suitably low in energy, at 633 and 558 keV in $^{188}$Os and $^{190}$Os, respectively.[1] In $^{189}$Os one would then expect to see two bands with $K = |K_0 \pm 2|$ about 600 keV above each $K_0$ quasiparticle band. (The $K_0 - 2$ somewhat lower and the $K_0 + 2$ somewhat higher in energy.)

In the simplest picture, a pure vibrational state should have zero cross section for transfer reactions.[61] However, there have already been many observations of vibrational states being populated in deformed nuclei by the $(d,p)$ and $(d,t)$ reactions.[60,62,63]

A more sophisticated theory of vibrational states has been set forth by Bes and Cho[64] and by Soloviev *et al.*[65] They have calculated odd-$A$ wave functions microscopically, treating a phonon as a linear combination of two-quasiparticle states. Unfortunately their calculations did not include the Os isotopes. They have obtained estimates of the (usually small) one-quasiparticle admixture in mainly vibrational states, and vice versa. Transfer cross sections should be a measure of single particle admixture.

The selection rules[57] for strong mixing of a Nilsson state with a vibration built on another Nilsson state are $\Delta N = \Delta n_z = 0$, $\Delta K = \Delta\Lambda = \pm 2$. The pairs of states $\frac{1}{2}[510], \frac{3}{2}[512]$ and $\frac{5}{2}[503], \frac{9}{2}[505]$ satisfy those rules. Of course, the interaction is strongest when the unperturbed energies are

closest.

In the following discussion, vibrational band members will be denoted $IK(K_0[Nn_z\Lambda])$. For example, $\frac{5}{2}\frac{3}{2}(\frac{7}{2}[503])$ would be the $\frac{5}{2}-$ member of the $K_0-2\ \gamma$ band built on the $\frac{7}{2}[503]$ Nilsson state.

The $\frac{5}{2}-$ level at 276 keV could be the bandhead of the $K_0-2$ vibration built on the $\frac{9}{2}[505]$. The deexcitation branching of this state is shown in Fig. 7. By far the strongest transition depopulating the 276 keV $\frac{5}{2}-$ level connects it with the $\frac{9}{2}[505]$; this $\frac{5}{2}-\rightarrow\frac{9}{2}-$ transition probably is a collective deexcitation, which would be favored over transitions between single particle bands. Mixing between the high lying $\frac{5}{2}\frac{5}{2}[503]$ particle state and the $\frac{5}{2}\frac{5}{2}(\frac{9}{2}[505])$ would lower the energy of the latter, and could account for part of the $(d,p)$ but not the $(d,t)$ cross section of the 276 keV level. Coupling with $\frac{5}{2}-$ members of vibrational bands built on the $\frac{1}{2}[510]$ and $\frac{3}{2}[512]$ could further depress the $\frac{5}{2}\frac{5}{2}(\frac{9}{2}[505])$, but there is no obvious reason why this should be the only vibrational state to lie so far below the phonon energy. Mixing of the $\frac{5}{2}\frac{5}{2}(\frac{9}{2}[505])$ with the $\frac{5}{2}\frac{3}{2}[512]$ should be weak, but this is a possible additional source of observed neutron transfer intensity to the 276 keV level; $\gamma$-ray transitions (Fig. 7) to members of the $\frac{3}{3}[512]$ band also indicate that there is some interaction. The 276 keV state, then, seems to be an anomalous state. Within the framework of the axially symmetric Nilsson model it contains a considerable amount of $\frac{5}{2}\frac{5}{2}(\frac{9}{2}[505])$ collective character but also has an appreciable amount of quasiparticle character from uncertain sources. This interpretation of the 276 keV state does not explain why it lies so low in energy, however.

The $K_0+2$ bands built on the $\frac{9}{2}[505]$ and $\frac{7}{2}[503]$ would have high spins and no source of transfer intensity, so they certainly would not have been seen in these experiments.

The $\frac{3}{2}\frac{3}{2}(\frac{7}{2}[503])$ might be expected to be populated in the $(n,\gamma)$ reaction. But of the unidentified low spin levels seen in the high energy $\gamma$-ray spectrum at 439, 506, 550, and 558 keV none decays to the

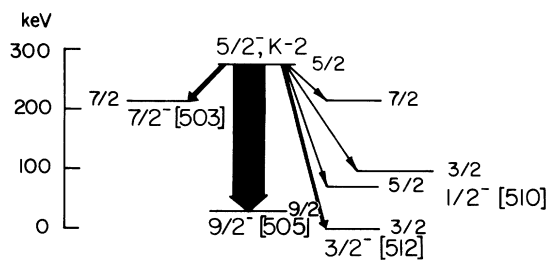


FIG. 7. Deexcitation of the 276 keV $\frac{5}{2}-$ level in $^{189}$Os. Widths of the arrows represent the $\gamma$-ray intensities measured in $^{189}$Ir decay (Ref. 33).

217 keV $\frac{7}{2}\frac{7}{2}[503]$ state. There is an $l=1$ state at 600 keV which might be a candidate for the $\frac{3}{2}\frac{3}{2}(\frac{7}{2}[503])$ assignment, but it is one of the strongest states in the transfer spectra. By mixing, it would borrow some of the enormous $(d,p)$ strength of the $\frac{3}{2}\frac{3}{2}[501]$, but there is no obvious source of $(d,t)$ strength. There is no experimentally observed level which can clearly be assigned as the $\frac{3}{2}\frac{3}{2}(\frac{7}{2}[503])$.

There is a multitude of possible interactions for the $\frac{1}{2}[510]$ and $\frac{3}{2}[512]$ orbitals. First, the quasiparticle bands themselves mix strongly. Second, each quasiparticle band can mix with the $K_0-2\ \gamma$ vibrational band of the other, according to the strong rules for particle-vibrational coupling. Third, Coriolis mixing can occur between the two $K_0-2\ \gamma$ vibrational bands. Fourth, there can be many interactions with higher lying Nilsson states. With so much mixing, then, it is not surprising that no recognizable rotational pattern could be observed for any of the vibrational excitations.

Strong mixing of the $\frac{3}{2}\frac{1}{2}(\frac{3}{2}[512])$ with the $\frac{3}{2}\frac{3}{2}(\frac{1}{2}[510])$ should elevate the former and depress the latter. There is no analogous interaction for the $\frac{1}{2}\frac{1}{2}(\frac{3}{2}[512])$. All three of these states can acquire transfer strength by mixing with the base states. Therefore, it would seem reasonable to assign the low spin states at 439, 506, and 558 keV as the $\frac{3}{2}\frac{3}{2}(\frac{1}{2}[510])$, the $\frac{1}{2}\frac{1}{2}(\frac{3}{2}[512])$, and the $\frac{3}{2}\frac{1}{2}(\frac{3}{2}[512])$, respectively. Several observations have bearing on these assignments. All three of these states are populated by inelastic scattering, the 506 keV level most strongly.[3] The observed inelastic scattering would be expected if the two $\frac{3}{2}-$ states are mixed, so that both are then related to the ground state. As is shown in Fig. 8, the $\gamma$-ray deexcitation of the 439, 506, and 558 keV states goes exclusively to members of the $\frac{3}{2}[512]$ and $\frac{1}{2}[510]$ bands, indicating close relationship among all these levels. Observation of the 67 keV transition connecting the 506 and 439 keV levels, when higher energy deexcitations would normally be favored, indicates that there may be a rotational relationship between the two levels. A strong $\frac{3}{2}\frac{1}{2}(\frac{3}{2}[512])$ admixture in the 439 keV state could account for the effect. Similar low energy deexcitations of the 558 keV level are less likely to be observed, since the level is less strongly populated than the 506 keV state. It is suggested, then, that the 439 and 558 keV each contain roughly equal amounts of $\frac{3}{2}\frac{3}{2}(\frac{1}{2}[510])$ and $\frac{3}{2}\frac{1}{2}(\frac{3}{2}[512])$ character, and that the $\frac{1}{2}\frac{1}{2}(\frac{3}{2}[512])$ state is at 506 keV.

Since the $M1$ transition probability within the $\frac{1}{2}-[510]$ band is much larger than the $M1$ within the $\frac{3}{2}-[512]$ band or the $M1\ \frac{1}{2}-[510]\rightarrow\frac{3}{2}-[512]$ transition, the tendency to populate the $\frac{1}{2}-[510]$ band beginning at 36 keV more strongly than the

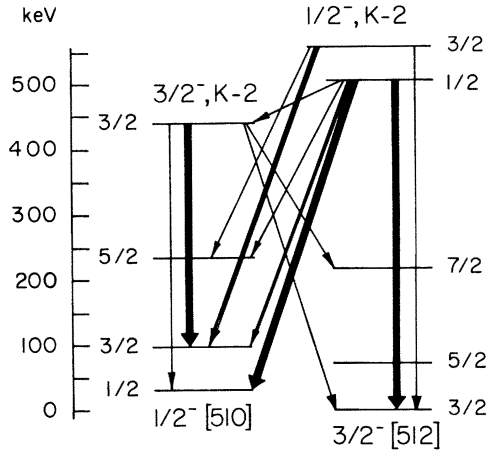


FIG. 8. Deexcitation of the proposed $K_0-2\gamma$ vibrational bands built upon the $\frac{3}{2}[512]$ and $\frac{1}{2}[510]$ states in $^{189}$Os. Widths of the arrows indicate roughly the $\gamma$-ray intensities observed in the $(n,\gamma)$ experiment, except for the 439 keV $\gamma$ ray which was observed only in $^{189}$Ir decay (Ref. 33).

$\frac{3}{2}-[512]$ band can be understood when the mixing described for the 439 and 506 keV bands is taken into account.

One would expect the $\frac{7}{2}\frac{7}{2}(\frac{3}{2}[512])$, as well as the 506 keV $\frac{1}{2}\frac{1}{2}(\frac{3}{2}[512])$, to be strongly populated in the $(d,d')$ reaction. A state has been observed at 733 keV in the $(d,d')$ spectrum, with about the same intensity as the 506 keV state,[3] which could be the $\frac{7}{2}\frac{7}{2}(\frac{3}{2}[512])$. A state at 735 keV in the $(d,t)$ spectra has been tentatively assigned in the previous section as the $\frac{3}{2}-$ member of the $\frac{1}{2}[521]$ band. If this assignment is correct, then the $(d,t)$ and $(d,d')$ probably populate different levels.

If the transfer cross section of vibrational states is a measure of the one-quasiparticle admixture, then the sum over the observed states should give approximately the expected total cross sections. However, for $^{189}$Os the assigned quasiparticle states already have about the expected cross sections. If the transfer strength of mainly collective states comes from higher Nilsson orbitals, then it is surprising that so many of the states (assigned and unassigned) above 400 keV have particle/hole character similar to states lying close to the Fermi energy, where $U^2$ and $V^2$ are about 0.5.

### D. Nilsson level scheme

The interpretation of the energy levels in $^{189}$Os is summarized in Fig. 9, which displays the levels grouped in rotational bands together with their possible associated vibrational excitations. In contrast with the single particle excitations, for which satisfactory assignments could be based upon semiquantitative agreement between experiment

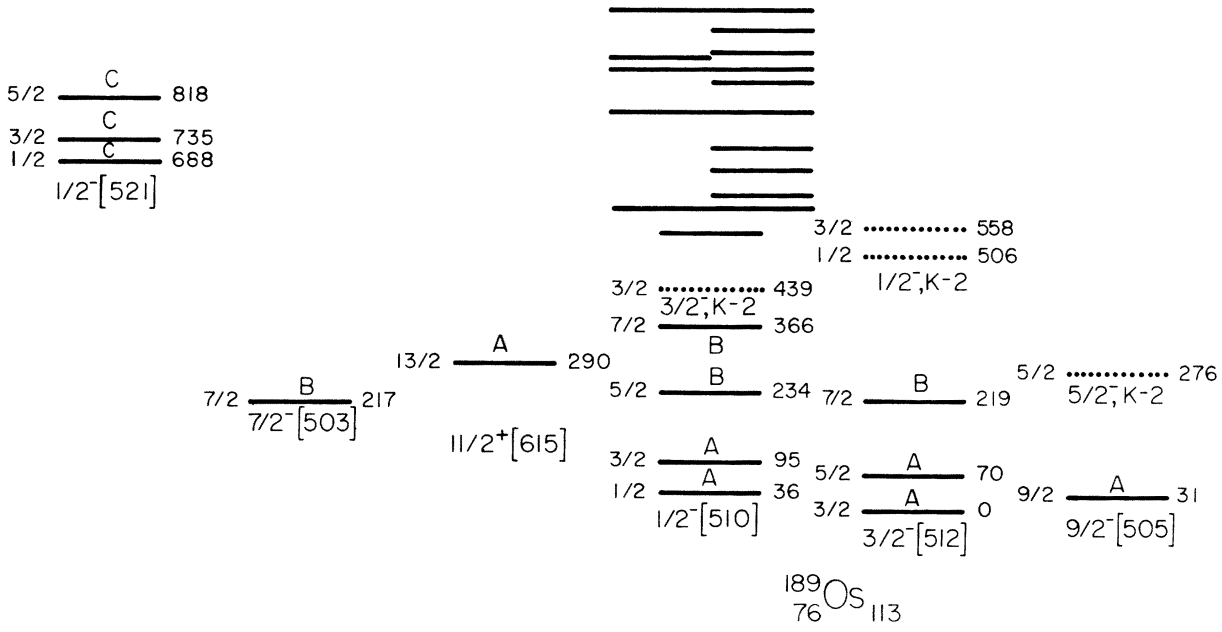


FIG. 9. Level assignments in $^{189}$Os. Hole states are shown to the left, and particle states to the right of the ground band. The degree of confidence for the Nilsson assignments is indicated by the letters A, B, and C, which designate certain, probable, and tentative identifications, respectively. Possible associated vibrational excitations are indicated as dotted lines. Unassigned levels below 1 MeV are also shown, with their particle or hole character indicated by horizontal position.

and theory, the identification of the vibrational states is far more speculative. The large number of levels seen above 400 keV makes the assignments less definite than at lower excitation energies. But the greatest difficulty in assigning vibrational states is due to the fact that their wave functions are not related in a simple way to neutron transfer.

## IV. DISCUSSION

### A. Nilsson orbital systematics

An important result of these studies is the systematic identification of low lying excited states which can be related to the Nilsson orbitals.[4,5,37] The properties of these states in $^{189}$Os deviate considerably from the predictions of the Nilsson model, probably largely because of the strong Coriolis interaction[52] expected for such weakly deformed nuclei.

The systematics of the Nilsson levels implies that with increasing odd neutron number at approximately constant deformation each Nilsson orbital in turn will first be observed as a high lying particle excitation and ultimately become an increasingly deeper hole excitation. In this simple picture each Nilsson orbital would be the ground state for only one odd value of $N$. These expectations hold true fairly generally in the rare earth region.[57] From the information available on other odd-$A$ Os nuclei,[1,2,66,67,59] together with the data of this experiment, it can be seen that this trend is not followed very well for $N>110$. In particular, the $\frac{1}{2}[510]$ and the $\frac{3}{2}-[512]$ states each occur within 100 keV of the ground state in four consecutive odd isotopes between $^{185}$Os and $^{193}$Os.

These unusual observations can probably be attributed to a decrease in deformation with increasing mass in the Os region. This effect can be visualized from an inspection of the Nilsson diagram for this mass region. As one proceeds along either the $\frac{1}{2}[510]$ or the $\frac{3}{2}[512]$ Nilsson state from larger toward smaller deformation, there are several high-$K$ orbitals from the $i_{13/2}$ and $h_{9/2}$ spherical states which cross below the $\frac{1}{2}[510]$. These high-$K$ orbitals, therefore, are more likely to be filled before the $\frac{1}{2}[510]$ in the less deformed heavier isotopes, thus enabling the $\frac{1}{2}[510]$ and $\frac{3}{2}[512]$ to remain at low excitation energy.

### B. Coriolis coupling and spherical transfer strength

In the $(d,p)$ and $(d,t)$ spectra observed in this work, the two dominant peaks at low excitation energy are those which have been assigned as the $\frac{3}{2}\frac{1}{2}[510]$ and $\frac{5}{2}\frac{3}{2}[512]$ states. From the pure Nilsson model calculations (Table VII) one would expect that the $\frac{3}{2}$ and $\frac{5}{2}$ members of both the $\frac{1}{2}[510]$ and the $\frac{3}{2}[512]$ bands should be populated, but, as was discussed earlier, the strengths of the four expected states are combined into only two by Coriolis coupling. According to the usual two-band Coriolis treatment,[52] then, it would be expected that the observed $\frac{5}{2}$ state should have at most the sum of the unperturbed $\frac{5}{2}$ strengths calculated for the two bands, and similarly the observed $\frac{3}{2}$ state should not be stronger than the calculated $\frac{3}{2}$ sum. However, the measurements definitely reveal transfer strengths larger than the predicted sums. Similarly excessive cross sections have been seen in $^{185}$W but not in the lighter W isotopes.[6] Apparently $^{187}$Os also exceeds the predicted $\frac{3}{2}$ and $\frac{5}{2}$ strength, although the two states were unresolved in the transfer spectra.[51]

The reason for the discrepancy in the transfer strength is probably the neglect of admixtures from other Nilsson orbitals. As deformation decreases toward the heavier Os isotopes, the unperturbed energies of the $\frac{3}{2}[501]$ and the $\frac{5}{2}[503]$ Nilsson states become lower, and also there is an increase in the inertial parameter $\hbar^2/2I$, which is the coupling constant for the Coriolis interaction. Both of these effects can strongly enhance the mixing of higher orbitals with the lowest lying states.

The experimentally observed cross section patterns can be viewed as indications of the increasing dominance of the Coriolis interaction with decreasing deformation. The Coriolis interaction tends to counteract the splitting of spherical transfer strength caused by the deformation of the nuclear potential, and thus tends to restore the cross section pattern expected for a spherical nucleus.

### C. Possible triaxiality in $^{189}$Os

It has long been recognized[7] that the heavy Os nuclei probably represent the closest approach of the experimental situation to the theoretical expectations of triaxiality. The great majority of effort in this region (both experimental and theoretical) has involved the even Os nuclei. These studies have usually revolved around the fact that the $K=2^+$ $\gamma$ vibrational band moves precipitously downward in energy as neutron number increases until it is almost degenerate with (but slightly higher than) the 4+ rotational member of the ground state band at $^{190}$Os, dropping below at $^{192}$Os. In the earliest and simplest models[7] the $\gamma$ band sequence implies a series of triaxial nuclei in which the $\gamma$ deformation increases until at $^{192}$Os the nucleus is more nearly oblate than prolate.

The preponderance of evidence, however, suggests that the quadrupole moments for all of the even Os nuclei are positive (including $^{192}$Os) whereas the quadrupole moments of all of the stable even Pt nuclei are negative including the isotopes of the heaviest Os nuclei. How close the potential functions of the Os nuclei come to $\gamma$ instability (in which the nucleus can take all $\gamma$ degrees of freedom in the $\beta$-$\gamma$ plane without change in potential energy) is not clear.

Since odd-$A$ Os nuclei have an additional particle which can act as a probe for the nuclear shape, it might be expected that this additional sensitivity might give important clues to possible triaxiality in the heavy Os nuclei. Unfortunately very little theoretical work has been done for odd nuclei with triaxial symmetry. In part, this is because the calculations are so difficult, but it can also be blamed on the shortage of experimental data needed to inspire theoretical calculations. The techniques which have been used for calculating the properties of odd triaxial nuclei[8-11] are difficult to use effectively for the present work because they involve unacceptable approximations; they provide no straightforward way of estimating transfer cross sections, and they can produce almost any spin sequence in a band by variation of a few parameters. However, a few states have been observed in $^{189}$Os which have features resembling those predicted for specific rotational levels of a triaxial rotor.

Of particular interest is the behavior predicted by Pashkevich[8,68] and Meyer-ter-Vehn[11,69,70] for the first rotational state with spin $j-2$, associated with an intrinsic single hole state in a $j>\frac{3}{2}$ shell. The first $j-2$ state lies at fairly high excitation energy for a prolate nucleus, but drops sharply as $\gamma$ increases from 10° to 30°, becoming the lowest state above the bandhead for $\gamma>30°$. The reduced $E2$ probability for the transition, connecting this first $j-2$ state with the $j$ bandhead, increases abruptly by two to three orders of magnitude around $\gamma=10°$, where the $j-2$ state begins to drop in excitation energy.

The behavior of the $j-2$ state described above very strongly resembles that of the $\frac{5}{2}-$ state observed at 276 keV in $^{189}$Os. This $\frac{5}{2}-$ state deexcites selectively by an $E2$ transition[30,33] to the $\frac{9}{2}-[505]$ bandhead, and lies too low in energy to be a typical vibrational excitation. This behavior provides rather strong evidence for triaxial symmetry in $^{189}$Os. Perhaps even stronger evidence would be a measured $E2$ transition probability characteristic of a rotational 245 keV $\frac{5}{2}-\rightarrow\frac{9}{2}-$ transition. We hope the present experimental evidence will stimulate more sophisticated theoretical calculations.

## V. CONCLUSION

The addition of $(d,p)$, $(d,t)$, and $(n,\gamma)$ data presented here to the already extensive decay scheme data not only provides additional information and levels for the $^{189}$Os level structure, but also allows greater sophistication in the interpretation of these levels.

Clearly the Nilsson model is able to give a qualitative description of many of the low lying states in $^{189}$Os, but just as clearly the Nilsson model does not predict the properties of the transition nucleus $^{189}$Os as successfully as it does those of the more strongly deformed nuclei.

Among the emerging complexities observed in this study are (1) the anomalies in the Nilsson orbital systematics which may be qualitatively understood in terms of changing deformation and severe Coriolis coupling, (2) the anomalous $(d,p)$ and $(d,t)$ cross sections particularly for the $\frac{3}{2}-$ and $\frac{5}{2}-$ states which again qualitatively may be understood on the basis of increasing Coriolis coupling tending to restore the cross sections expected for a spherical nucleus and destroy that expected for the Nilsson model, and (3) the probable triaxiality associated with low lying states connected by collective transitions to known Nilsson states.

We believe these interesting deviations from the Nilsson model deserve further theoretical and experimental study and have undertaken the study of $^{191}$Os and $^{193}$Os in the hope that these more neutron rich nuclei will provide even more striking evidence for these phenomena.

## ACKNOWLEDGMENTS

We would like to thank Ken Chapman and the staff of the Florida State University tandem laboratory for their support in the $(d,p)$ and $(d,t)$ runs. Those who helped in operating the tandem and the spectrograph are J. W. Dawson, J. L. Dubard, K. G. Ellson, H. D. Jones, R. G. Lanier, M. M. Minor, R. L. Mlekodaj, T. J. Mulligan, Y. Shida, and R. C. Thompson. The spectrograph plates were meticulously scanned by Veronica Bryant Lanier, Mary Jones, Sue Hipps, and Ella Jean Wehunt. We thank K. E. Chellis for the Os targets and Edward T. Jurney and the staff of the Los Alamos Omega West reactor for making the $(n,\gamma)$ experiments possible. We are particularly grateful to Dr. N. Onishi for the theoretical calculations of the Nilsson levels in this paper.

†Supported by the U. S. Energy Research and Development Administration.

*Present address: Research Department, Squibb Pharmaceutical Co., New Brunswick, New Jersey 08903.

‡Present address: Nuclear Physics Department, KFA Jülich, D517 Jülich, West Germany.

[1]M. R. Schmorak, Nucl. Data Sheets 9, 195 (1973); 9, 401 (1973); 10, 553 (1974); 13, 267 (1974); C. M. Lederer, J. M. Hollander, and I. Perlman, *Table of Isotopes* (Wiley, New York, 1967), 6th ed.; M. B. Lewis, *ibid.* 12, 397 (1974).

[2]D. Benson, Jr., P. Kleinheinz, and R. K. Sheline, Nukleonika 20, 169 (1975).

[3]P. Morgen, Ph.D. thesis, Aarhus Universitet, 1969 (unpublished); P. Morgen, J. H. Onsgaard, B. S. Nielsen, and C. Sondergaard, Nucl. Phys. A252, 477 (1975).

[4]S. G. Nilsson, K. Dan. Vidensk. Selsk. Mat.-Fys. Medd. 29, No. 16 (1955).

[5]C. Gustafson, I. L. Lamm, B. Nilsson, and S. G. Nilsson, Ark. Fys. 36, 613 (1967).

[6]R. F. Casten, P. Kleinheinz, P. J. Daly, and B. Elbek, K. Dan. Vidensk. Selsk. Mat.-Fys. Medd. 38, No. 13 (1972).

[7]A. S. Davydov and G. F. Filippov, Nucl. Phys. 8, 237 (1958); A. S. Davydov and V. S. Rostovsky, *ibid.* 12, 58 (1959).

[8]V. V. Pashkevich and R. A. Sardaryan, Izv. Akad. Nauk. SSSR Ser. Fiz. 28, 1188 (1964). [Bull. Acad. Sci. USSR Phys. Ser. 28, 1088 (1964)].

[9]K. T. Hecht and G. R. Satchler, Nucl. Phys. 32, 286 (1962).

[10]L. W. Person and J. O. Rasmussen, Nucl. Phys. 36, 666 (1962).

[11]J. Meyer-ter-Vehn, F. S. Stevens, and R. M. Diamond, Phys. Rev. Lett. 32, 1383 (1974).

[12]C. P. Browne and W. W. Buechner, Rev. Sci. Instrum. 27, 899 (1956).

[13]R. G. Lanier, D. Benson, Jr., and M. M. Minor, Computer Code STRILDE, Florida State University, 1966 (unpublished).

[14]H. C. Kaufmann, computer code STRIP, Florida State University, 1966 (unpublished).

[15]R. A. Kenefick, Ph.D. dissertation, Florida State University, 1962 (unpublished).

[16]C. F. Moore and C. Watson, computer code HILDE, Technical Report No. 7, Tandem Accelerator Laboratory, Florida State University, 1965 (unpublished).

[17]C. L. Nealy, Ph.D. dissertation, Florida State University, 1965 (unpublished).

[18]E. T. Jurney, H. T. Motz, and S. H. Vegors, Jr., Nucl. Phys. A94, 351 (1967).

[19]J. B. Marion, Nucl. Data A4, 301 (1968).

[20]E. T. Jurney and H. T. Motz, in *International Conference on Nuclear Physics with Reactor Neutrons*, ANL-6797, edited by F. E. Throw (Argonne National Laboratory, Argonne, 1963), p. 241.

[21]L. V. Groshev, A. M. Demidov, V. I. Pelekhov, L. L. Sokolovskii, G. A. Bartholomew, A. Doveika, K. M. Eastwood, and S. Monaro, Nucl. Data A5, 243 (1969).

[22]T. Tamura, computer codes BEMAIN and DWMAIN, Oak Ridge National Laboratory, 1967 (unpublished); the optical parameters were taken directly from the potential DIPI used for $^{183}$W in R. H. Siemssen and J. R. Erskine, Phys. Rev. 146, 911 (1966).

[23]C. Maples, G. W. Goth, and J. Cerny, Nucl. Data A2, 429 (1966).

[24]M. A. Mariscotti, W. R. Kane, and G. T. Emery, in *Proceedings of the Conference on Slow Neutron Capture Gamma-Ray Spectroscopy*, ANL-7282, edited by F. E. Throw (Argonne National Laboratory Argonne, 1966), p. 19.

[25]E. Böhm and K. Stelzer, in *Proceedings of the International Symposium on Neutron Capture Gamma-Ray Spectroscopy, Studsvik* (International Atomic Energy Agency, Vienna, 1969), p. 403.

[26]W. McLatchie, S. Whinery, J. D. Camdougall, and H. E. Duckworth, Nucl. Phys. A145, 244 (1970).

[27]D. Benson, Jr., and E. T. Jurney (unpublished data).

[28]R. M. Diamond and J. M. Hollander, Nucl. Phys. 8, 143 (1958).

[29]B. Harmatz, T. H. Handley, and J. W. Milhelich, Phys. Rev. 128, 1186 (1962).

[30]B. Crasemann, G. T. Emery, W. R. Kane, and M. L. Perlman, Phys. Rev. 132, 1681 (1963).

[31]P. H. Blichert-Toft, Ark. Fys. 28, 415 (1965).

[32]A. Artna, Nucl. Data B1 (No. 2), 85 (1966).

[33]S. G. Malmskog, V. Berg, and A. Bäcklin, Nucl. Phys. A153, 316 (1970).

[34]R. B. Begzhanov, N. A. Il'khamdzhanov, A. I. Muminov, and P. S. Radzhanov, in *Proceedings of the XXI Annual Conference on Nuclear Spectroscopy and Structure of the Atomic Nucleus, Moscow* (Nauka, Leningrad, 1971), p. 129.

[35]A. Kerek, P. Kleinheinz, Th. Lindblad, R. H. Price, and B. S. Nielsen, Annual Report, Research Institute for Physics, Stockholm, 1971 (unpublished), p. 54.

[36]N. Onishi, computer code DFWF, Florida State University, 1969 (unpublished).

[37]S. G. Nilsson, C. F. Tsang, A. Sobiczewski, Z. Szymanski, S. Wycech, C. Gustafson, I. L. Lamm, P. Möller, and B. Nilsson, Nucl. Phys. A131, 1 (1969).

[38]G. Himmel, Z. Phys. 211, 68 (1968).

[39]K. E. G. Löbner, M. Vetter, and V. Hönig, Nucl. Data A7, 495 (1970).

[40]A. M. Lane, *Nuclear Theory: Pairing Force Correlations and Collective Motion* (Benjamin, New York, 1964).

[41]W. Ogle, S. Wahlborn, R. Piepenbring, and S. Fredrickson, Rev. Mod. Phys. 43, 424 (1971).

[42]B. Elbek and P. O. Tjøm, *Advances in Nuclear Physics*, edited by M. Baranger and E. Vogt (Plenum, New York, 1969), Vol. 3, p. 259.

[43]W. Tobocman, *Theory of Direct Nuclear Reactions* (Oxford U. P., Oxford, 1961).

[44]R. H. Siemssen and J. R. Erskine, Phys. Rev. Lett. 19, 70 (1967).

[45]C. M. Perey and F. G. Perey, Phys. Rev. 132, 755 (1963); see also F. G. Perey, *ibid.* 131, 745 (1963).

[46]G. H. Fuller and V. M. Cohen, Nucl. Data A5, 433 (1969).

[47]D. H. Rester, M. S. Moore, F. E. Durham, and C. M. Class, Nucl. Phys. 22, 104 (1961).

[48]F. K. McGowan, R. L. Robinson, P. H. Stelson, and J. L. C. Ford, Jr., Bull. Am. Phys. Soc. 8, 548 (1973); ORNL Report No. ORNL-3425, 1963 (unpublished) p. 26.

[49]A. Z. Hrynkiewicz, B. Sawicka, J. Styczen, S. Szymczyk, and M. Szawlowski, Acta Phys. Pol. 31, 437 (1967).
[50]J. R. Erskine, Phys. Rev. 138, B66 (1965).
[51]P. Morgen, B. S. Nielsen, J. Onsgaard, and C. Sondergaard, Nucl. Phys. A204, 81 (1973); R. Thompson and R. K. Sheline, Phys. Rev. C 7, 1247 (1973).
[52]A. K. Kerman, K. Dan. Vidensk. Selsk. Mat.-Fys. Medd. 30, No. 15 (1956).
[53]R. F. Casten, P. Kleinheinz, P. J. Daly, and B. Elbek, Phys. Rev. C 3, 1271 (1971).
[54]G. Scharff-Goldhaber, D. E. Alburger, G. Harbottle, and M. McKeown, Phys. Rev. 111, 913 (1958).
[55]S. G. Nilsson, K. Dan. Vidensk. Selsk. Mat.-Fys. Medd. 29, No. 16 (1955).
[56]F. Wagner, G. Kaindl, H. Bohn, U. Biebl, H. Schaller, and P. Kienle, Phys. Lett. 28B, 548 (1969).
[57]M. E. Bunker and C. W. Reich, Rev. Mod. Phys. 43, 348 (1971).
[58]P. Kleinheinz, R. F. Casten, and B. Nilsson, Nucl. Phys. A203, 539 (1973).
[59]Y. A. Ellis, Nucl. Data Sheets 14, 347 (1975).
[60]R. K. Sheline, W. N. Shelton, H. T. Motz, and R. E. Carter, Phys. Rev. 136, B351 (1964).
[61]G. R. Stachler, Ann. Phys. (N.Y.) 3, 275 (1958).
[62]D. G. Burke, B. Zeidman, B. Elbek, B. Herskind, and J. Olesen, K. Dan. Vidensk. Selsk. Mat. Fys. Medd. 35, No. 2 (1966).
[63]F. A. Rickey and R. K. Sheline, Phys. Rev. 170, 1157 (1968).
[64]D. R. Bes and Cho Yi-Chung, Nucl. Phys. 86, 581 (1966).
[65]V. G. Soloviev and P. Vogel, Nucl. Phys. A92, 449 (1967); V. G. Soloviev, P. Vogel, and G. Jungclaussen, Izv. Akad. Nauk SSSR Ser. Fiz. 31, 515 (1967) [Bull. Acad. Sci. USSR Phys. Ser. 31, 515 (1967)].
[66]K. Ahlgren and P. J. Daly, Nucl. Phys. A189, 368 (1972).
[67]H. Sodan, W. D. Fromm, L. Funke, P. Kemnitz, K. H. Kaun, and G. Winter, Annual Report, Zentralinstitut für Kernforschung, Rossendorf, 1972 (unpublished), p. 99.
[68]V. V. Pashkevich, Izv. Akad. Nauk SSSR Ser. Fiz. 30, 257 (1966) [Bull. Acad. Sci. USSR Phys. Ser. 30, 262 (1966)].
[69]J. Meyer-ter-Vehn, Nucl. Phys. A249, 111 (1975).
[70]J. Meyer-ter-Vehn, Nucl. Phys. A249, 141 (1975).